Contribution from the Institut für Organische Chemie der Friedrich-Alexander-Universität Erlangen-Nürnberg, Henkestrasse 42, D-8520 Erlangen, Federal Republic of Germany

The Anomeric Effect with Central Atoms Other Than Carbon. 2. Strong Interactions between Nonbonded Substituents in Mono- and Polyfluorinated First- and Second-Row Amines, $F_nAH_mNH_2$

Alan E. Reed* and Paul von Ragué Schleyer

Received December 11, 1987

Full geometry optimizations at the HF/6-31G* level of ab initio theory have been carried out for the conformers and inversion and rotation transition structures of the mono- and polyfluorinated amines $F_nAH_mNH_2$ (A = Be, B, C, N, O, Mg, Al, Si, P, S). For the two molecules whose structures have been determined experimentally (F_2BNH_2 and F_2PNH_2), good agreement is obtained. Significant conformational dependencies of the A–N and A–F bond lengths, degree of pyramidalization of the NH_2 group, FAN angle, and F–NH_2 interaction energy (eq 1) have been found. These trends are in accordance with the generalized anomeric effect and are explainable in terms of $n_N \rightarrow \sigma_{AF}^*$ negative hyperconjugation. The full magnitude of the $n_N \rightarrow \sigma_{AF}^*$ interactions is masked partially in many cases by $n_N \rightarrow \sigma_{AH}^*$ hyperconjugation. A detailed study of $FSNH_2$ with natural bond orbital (NBO) analysis shows that the particularly strong generalized anomeric effect in $FSNH_2$ (lengthening of the S–N bond by 0.10 Å during internal rotation with an associated barrier of 18 kcal/mol) can be explained quantitatively in terms of $n_N \rightarrow \sigma_{SF}^*$ hyperconjugation. The related molecule $ClSNH_2$ has also been investigated, where strong $n_N \rightarrow \sigma_{SCl}^*$ interaction leads to an internal rotation barrier of 16 kcal/mol. This value is in the range of experimentally determined barriers for analogous sulfenamides. In all of the species studied, $n_N \rightarrow d_A$ bonding with d orbitals on atom A is found to be qualitatively unimportant in comparison with $n_N \rightarrow \sigma_{AX}^*$ interactions.

I. Introduction

The influence of stereoelectronic interactions on molecular conformation, energies, and reactivity is being increasingly recognized and experimentally exploited.[1] The central and unifying stereoelectronic interaction is the generalized anomeric effect.[1,2] The anomeric effect was first discovered in carbohydrate chemistry through the observation that oxygen substituents sometimes prefer positions that, on purely *steric* grounds, are less favorable (i.e., axial instead of equatorial positions on certain six-membered heterocyclic systems).[3] However, the anomeric effect is a quite general phenomenon and is restricted neither to cyclic systems nor to carbon centers. It also has been associated with the "gauche effect"[4] and the progressive increase in C–F bond strength with increased fluorine substitution in the fluoromethane series.[1a,2] The *generalized* anomeric effect results in the stabilization of conformations of YAX moieties where one of the lone pairs of atom Y (in the case of O and S, the π-type lone pair) is antiperiplanar to the AX bond, A being the central atom and X an atom more electronegative than A:

Associated with this (often sterically less favorable) conformational preference is a shortening and strengthening of the A–Y bond and a lengthening and weakening of the A–X bond. A wealth of evidence indicates that such stereospecific stabilizing interactions are often important in transition-state structures and influence the course of chemical reactions involving such functional groups as acetals, esters, amides, phosphate esters, and double and triple bonds.[1] Stereoelectronic influences on reactivity and binding are certainly also important in biochemistry.[1] Indeed, it appears that the anomeric effect[2e] is used to strategic advantage by enzymes in order to selectively make certain bonds more labile.[1] The experimentally discovered anomeric effect is also mirrored by theoretical calculations;[1,2] cases have been found where the anomeric effect is so strong that it leads to the rupture of the A–X bond: the C–F bond in $FCH_2CH_2^-$[5] and the C–C bond in a strained bicyclic ring system with "push–pull" substituents.[6] The origin of the unusually short A–Y bond lengths in the "hypervalent" species F_3NO and F_3CO^- also can be associated with the generalized anomeric effect.[7]

Ab initio theory offers an excellent framework for systematically examining the strength of the generalized anomeric effect with respect to variation of the atoms Y, A, and X and, furthermore, for testing quantitatively the reasonableness of the various proposed explanations. Thus far we have completed studies of two series of X_nAH_mY species. In the first, we fixed A = C (carbon) and n = 1 and varied the groups X and Y.[2b] In the second, we fixed X = Y = F (fluorine) and varied A and n.[2c] (All atoms from the first two rows of the periodic table were employed for A.) The former study[2b] showed that the strongest anomeric effect at carbon occurred with the combination X = F and Y = NH_2. Hence, we have employed this combination in the present study of the anomeric effect as a function of A and n. The NH_2 group has the additional advantage of possessing only one lone pair, which can be oriented at specific dihedral angles with respect to the A–F bonds. In contrast, there is the complicating factor with OH of σ and π lone pairs, and with F no dihedral angle can be defined. The choice of Y = NH_2 also affords the opportunity to study the

(1) The major comprehensive reviews of this field are the following: (a) Kirby, A. J. *The Anomeric Effect and Related Stereoelectronic Effects at Oxygen*; Springer: Berlin, 1983. (b) Deslongchamps, P. *Stereoelectronic Effects in Organic Chemistry*; Pergamon: New York, 1983. (c) Gorenstein, D. G. *Chem. Rev.* **1987**, *87*, 1047–1077.

(2) Leading references to the extensive literature in this area may be found in ref 1 and 3b and in other papers in this series on anomeric effects: (a) Schleyer, P. v. R.; Kos, A. J. *Tetrahedron* **1983**, *39*, 1141–1150. (b) Schleyer, P. v. R.; Jemmis, E. D.; Spitznagel, G. W. *J. Am. Chem. Soc.* **1985**, *107*, 6393–6394. (c) Reed, A. E.; Schleyer, P. v. R. *J. Am. Chem. Soc.* **1987**, *109*, 7362–7373. (d) Reed, A. E.; Schade, C.; Schleyer, P. v. R.; Kamath, P. V.; Chandrasekhar, J. *J. Chem. Soc., Chem. Commun.* **1988**, 67–69. (e) For brevity, we shall often employ the term "anomeric effect" even though the generalized anomeric effect is usually meant. Also see: Apeloig, Y.; Sanger, A. *J. Organomet. Chem.* **1988**, *346*, 305–313. Apeloig, Y.; Karni, M. *J. Chem. Soc., Perkin Trans. II* **1988**, 625–636.

(3) (a) Edward, J. T. *Chem. Ind.* (*London*) **1955**, 1102. (b) *Anomeric Effect, Origin and Consequences*; Szarek, W. A., Horton, D., Eds.; ACS Symposium Series 87; American Chemical Society: Washington, DC, 1979.

(4) Wolfe, S. *Acc. Chem. Res.* **1972**, *5*, 102–111.

(5) Bach, R. D.; Badger, R. C.; Lang, T. L. *J. Am. Chem. Soc.* **1979**, *101*, 2845–2848. See also ref 2a.

(6) (a) Ōsawa, E.; Ivanov, P. M.; Jaime, C. *J. Org. Chem.* **1983**, *48*, 3990–3992. (b) For an interesting experimental example involving equilibria between keto acids and hydroxylactones that are strongly influenced by the anomeric effect, see: Chadwick, D. J.; Dunitz, J. D. *J. Chem. Soc., Perkin Trans. 2* **1979**, 276–284.

(7) (a) Eyermann, C. J.; Jolly, W. L.; Xiang, S. F.; Shreeve, J. M.; Kinkead, S. A. *J. Fluorine Chem.* **1983**, *23*, 389–397. (b) Farnham, W. B.; Smart, B. E.; Middleton, W. J.; Calabrese, J. C.; Dixon, D. A. *J. Am. Chem. Soc.* **1985**, *107*, 4565–4567. (c) Farnham, W. B.; Dixon, D. A.; Calabrese, J. C. *J. Am. Chem. Soc.* **1988**, *110*, 2607–2611.

0020-1669/88/1327-3969$01.50/0

interplay between the anomeric effect and the degree of pyramidalization at nitrogen.

The classic explanation of the anomeric effect involves double-bond–no-bond resonance (or simply no-bond resonance), which, in a localized orbital interaction picture, corresponds to vicinal lone pair–antibond ($n_Y \rightarrow \sigma_{AX}^*$) delocalization.[1,2,8] Thus, the anomeric effect is a consequence of the departure from an ideally localized Lewis structure through negative hyperconjugation. This model is not universally accepted. Other workers prefer rationalizations based on electrostatic[9] or exchange repulsion[10] effects or the concepts called "σ-conjugation"[11] and "forbiddenness-reduction".[12] Due to its simplicity and emphasis on stabilizing orbital interactions, the negative hyperconjugation explanation is the one most preferred by experimentalists.[1] Therefore, it is important to investigate the extent to which the anomeric effect can be interpreted in terms of a negative hyperconjugation, $n \rightarrow \sigma^*$ delocalization model. One of our previous studies[2c] used natural bond orbital (NBO) analysis[13] for this purpose, a method that is derived from the Brunck–Weinhold[14] study on internal rotation barriers mentioned below. The NBO method is ideally suited for describing molecular wave functions in terms of Lewis structures and departures therefrom. The progressive energetic stabilization of fluorinated hydrides with increasing fluorine substitution was found to be described well in terms of $n \rightarrow \sigma^*$ interactions.[2c]

In considering the $F_nAH_mNH_2$ species in terms of $n_N \rightarrow \sigma_{AF}^*$ interactions, it is important to realize that $n_N \rightarrow \sigma_{AH}^*$ interactions, though weaker, occur as well; these act to partially mask the full effects of the $n_N \rightarrow \sigma_{AF}^*$ interactions. Consequences of $n_N \rightarrow \sigma_{CH}^*$ hyperconjugation are "methyl tilt" in H_3CNH_2,[15] Bohlmann bands (which refer to the IR spectral features associated with a lower C–H stretching frequency of C–H bonds that are trans to a nitrogen lone pair),[16] and the experimental observation of the delocalization of the nitrogen lone pair onto the trans hydrogen in H_3CNH_2 through (e,2e) spectroscopy.[17] Of the $F_nAH_mNH_2$ species to be studied in this work, $FSNH_2$ is the best candidate for quantitative analysis, as no σ_{AH}^* orbital is present and the $n_N \rightarrow \sigma_{SF}^*$ interaction can be expected both to dominate over all other delocalizations and to be large in magnitude: There is only one antibond with which the nitrogen lone pair can interact (thus, the $n_N \rightarrow \sigma_{SF}^*$ interaction can be turned off fully by internal rotation), and the SF bond is quite polar, making σ_{SF}^* a strong electron acceptor. We therefore single out $FSNH_2$ for detailed analysis, using the NBO method.

Very few of the species treated in this work have been studied previously, either experimentally or computationally. Lovas and Johnson made F_2BNH_2 in 1973 in the gas phase and determined its structure by microwave spectroscopy.[18] This molecule has been studied recently also by photoelectron spectroscopy[19] and by ab initio calculation.[19] F_2PNH_2, first synthesized in 1970 by Smith and Cohn,[20] was found by microwave spectroscopy to have a planar NH_2 group.[21] This was the first primary amine shown to be planar at N in the gas phase.[21] The planarity was attributed to bonding of the nitrogen lone pair with d orbitals on phosphorus. Boggs and Niu[22] have done computations on F_2PNH_2, but only results concerning the basis set dependence of the planarity at nitrogen were presented. Klöter et al.[23] succeeded in synthesizing F_3CNH_2 in 1977, which later was examined theoretically at the double-ζ basis set level by Heaton and Mills[24a] and, in a general study of CF_3 hyperconjugation, by Magnusson.[24b] Radom, Hehre, and Pople[25] included FCH_2NH_2, $FNHNH_2$, and $FONH_2$ in their classic work on rigid rotation barriers at the minimal basis set level. They presented Fourier analyses of the rotation barriers, assigning dipole–dipole and $n_N \rightarrow \sigma_{AF}^*$ hyperconjugation interactions as the origin of the V_1 and V_2 terms, respectively. (The periodicities of the V_1 and V_2 Fourier terms are 360 and 180°, respectively.) This assignment is somewhat misleading, however, because the V_2 term is by definition strictly equal for syn and anti orientations of the n_N and σ_{AF}^* orbitals with respect to each other. Since then, it has been recognized that $n_N \rightarrow \sigma_{AF}^*$ overlap is larger in magnitude for anti than for syn orientations of the n_N and σ_{AF}^* orbitals.[26] Therefore, $n_N \rightarrow \sigma_{AF}^*$ interactions will contribute to both the V_1 and V_2 terms. Brunck and Weinhold[14] showed from semiempirical calculations that removal of the antibonding orbitals in FCH_2NH_2, $FNHNH_2$, and $FONH_2$ (which prevents hyperconjugation from taking place) results in almost complete disappearance of their internal rotation barriers. They discussed their results also in relation to the anomeric effect. Pross and Radom[27] have discussed FCH_2NH_2 in relation to hyperconjugation, performing partial 4-31G optimizations. They found the C–N bond shortening in FCH_2NH_2 to be due to a combination of hyperconjugation and electrostatic (charge withdrawal) effects. We also have examined this species,[2a,b] as have Kost and Raban.[28a] The rotation–inversion activation barriers of two alkyl-substituted fluoroamines FCH_2NR_2 have been recently determined by Rahman et al.;[29] these were interpreted in relation to negative hyperconjugation. Though $FSNH_2$ is unknown, very large internal rotation barriers in $ClSNR_2$ species have been established,[28b,c] hence, we include $ClSNH_2$ in our study. This also makes possible a comparison between chlorinated and fluorinated amines.

II. Methods

The generalized anomeric effect in the $F_nAH_mNH_2$ series was studied

(8) Albright, T. A.; Burdett, J. K.; Whangbo, M.-H. *Orbital Interactions in Chemistry*; Wiley: New York, 1985; pp 171–182.
(9) Eliel, E. L.; Allinger, N. L.; Angyal, S. J.; Morrison, G. A. *Conformational Analysis*; American Chemical Society: Washington, DC, 1981.
(10) Smits, G. F. Ph.D. Thesis, University of Leiden, 1985. Smits, G. F.; Krol, M. R.; Altona, C. to be submitted for puiblication. Smits, G. F.; Altona, C. *Theor. Chim. Acta* **1985**, *67*, 461–475. See also ref 2c for discussion.
(11) Dewar, M. J. S. *J. Am. Chem. Soc.* **1984**, *106*, 669–682.
(12) Epiotis, N. D. *Lect. Notes Chem.* **1983**, *34*, 151–185. See also ref 2c for discussion.
(13) (a) Foster, J. P.; Weinhold, F. *J. Am. Chem. Soc.* **1980**, *102*, 7211–7218. (b) Reed, A. E.; Weinstock, R. B.; Weinhold, F. *J. Chem. Phys.* **1985**, *83*, 735–746. (c) Reed, A. E.; Weinhold, F. *J. Chem. Phys.* **1985**, *83*, 1736–1740. (d) Curtiss, L. A.; Pochatko, D. J.; Reed, A. E.; Weinhold, F. *J. Chem. Phys.* **1985**, *82*, 2679–2687. (e) Reed, A. E.; Curtiss, L. A.; Weinhold, F. *Chem. Rev.*, in press.
(14) Brunck, T. K.; Weinhold, F. *J. Am. Chem. Soc.* **1979**, *101*, 1700–1709.
(15) Pross, A.; Radom, L.; Riggs, N. V. *J. Am. Chem. Soc.* **1980**, *102*, 2253–2259.
(16) (a) Bohlmann, F. *Angew. Chem.* **1957**, *69*, 641–642; *Chem. Ber.* **1958**, *91*, 2157. (b) Hamlow, H. P.; Okuda, S.; Nakagawa, N. *Tetrahedron Lett.* **1964**, *37*, 2553–2559. (c) Krueger, P. J.; Jan, J.; Wieser, H. *J. Mol. Struct.* **1970**, *5*, 375–387. (d) Ernstbrunner, E. E.; Hudec, J. *J. Mol. Struct.* **1973**, *17*, 249–256.
(17) Tossel, J. A.; Lederman, S. M.; Moore, J. H.; Coplan, M. A.; Chornay, D. J. *J. Am. Chem. Soc.* **1984**, *106*, 976–979.
(18) Lovas, F. J.; Johnson, D. R. *J. Chem. Phys.* **1973**, *59*, 2347–2353.
(19) (a) Binkley, J. S., calculations quoted in ref 19b. (b) Thorne, L. R.; Gwinn, W. D. *J. Am. Chem. Soc.* **1982**, *104*, 3822–3827. (c) Ha, T.-K. *J. Mol. Struct.* **1986**, *136*, 165–176. (d) Kingsmill, C. A.; Werstiuk, N. H.; Westwood, N. P. C. *J. Am. Chem. Soc.* **1987**, *109*, 2870–2875.
(20) Smith, J. E.; Cohn, K. *J. Am. Chem. Soc.* **1970**, *92*, 6185–6186.
(21) Brittain, A. H.; Smith, J. E.; Lee, P. L.; Cohn, K.; Schwendeman, R. H. *J. Am. Chem. Soc.* **1971**, *93*, 6772–6776.
(22) Boggs, J. E.; Niu, Z. *J. Comput. Chem.* **1985**, *6*, 46–55.
(23) (a) Klöter, G.; Lutz, W.; Seppelt, K.; Sundermeyer, W. *Angew. Chem.* **1977**, *89*, 754. (b) Klöter, G.; Seppelt, K. *J. Am. Chem. Soc.* **1979**, *101*, 347–349. (c) Other perfluorinated organic primary amines (and imines) have been recently synthesized; see: Leidinger, W.; Sundermayer, W. *Chem. Ber.* **1982**, *115*, 2892–2897.
(24) (a) Heaton, M. M.; Mills, D. *Int. J. Quantum Chem.* **1985**, *28*, 163–180. (b) Magnusson, E. *J. Am. Chem. Soc.* **1986**, *108*, 11–16; *Aust. J. Chem.* **1986**, *39*, 747–755.
(25) Radom, L.; Hehre, W. J.; Pople, J. A. *J. Am. Chem. Soc.* **1972**, *94*, 2371–2381.
(26) See, e.g., ref 2c, 8, and 14. The reason for this is that, although the overlap between n_N and the hybrid orbital contribution to σ_{AF}^* from atom A is positive (leading to π_{AN} bonding), the overlap between n_N and the hybrid orbital contribution to σ_{AF}^* from F is negative. The former, positive overlap is rather similar at syn and anti conformations, but the latter, negative overlap is much larger in magnitude at the syn conformation. This leads to a much smaller positive net n_N–σ_{AF}^* overlap for syn than for anti.
(27) Pross, A.; Radom, L. *J. Comput. Chem.* **1980**, *1*, 295–300.
(28) (a) Kost, D.; Raban, M. *J. Am. Chem. Soc.* **1982**, *104*, 2960–2967. (b) Raban, M.; Kost, D. *Tetrahedron* **1984**, *40*, 3345–3381. (c) Dorie, J.; Gouesnard, J.-P. *J. Chim. Phys. Phys.-Chim. Biol.* **1984**, *81*, 15–19.
(29) Rahman, M. M.; Lemal, D. M.; Daily, W. P. *J. Am. Chem. Soc.* **1988**, *110*, 1964–1966.

Table I. Summary of HF/6-31G* Geometries and Energies for First-Row $F_nAH_mNH_2$ Species[a]

	sym	conformn	E[b]	E_{rel}	R(AN)	R(AF)	$\Delta\theta$(N)[c]	θ(FAN)[d]
$HBeNH_2$[e]	C_{2v}	P-pl	−70.849 87 (0)	0.00	1.503	1.337[f]	0.0	180.0
$FBeNH_2$	C_{2v}	P-pl	−169.805 11 [0]	0.00	1.506	1.377	0.0	180.0
H_2BNH_2	C_{2v}	A-pl	−81.435 18 (2)	33.83	1.457	1.200[f]	0.0	121.7
H_2BNH_2[e]	C_s	A-st	−81.442 19 (1)	29.44	1.471	1.200, 1.193[f]	35.8	122.1, 120.0
H_2BNH_2[e]	C_{2v}	P-pl	−81.489 10 (0)	0.00	1.389	1.193[f]	0.0	119.4
$FBHNH_2$	C_s	A-pl	−180.380 41 [2]	24.52	1.441	1.322	0.0	120.8
$FBHNH_2$	C_s	S-st	−180.384 50 [1]	21.96	1.455	1.315	29.7	119.4
$FBHNH_2$	C_s	A-st	−180.384 80 [1]	21.76	1.455	1.324	29.5	121.0
$FBHNH_2$	C_s	P-pl	−180.419 49 [0]	0.00	1.391	1.330	0.0	119.3
F_2BNH_2	C_{2v}	A-pl	−279.320 34 [2]	20.48	1.432	1.316	0.0	122.8
F_2BNH_2	C_s	A-st	−279.323 82 [1]	18.30	1.447	1.318, 1.310	27.2	123.1, 121.6
F_2BNH_2	C_{2v}	P-pl	−279.352 98 [0]	0.00	1.392	1.320	0.0	121.2
H_3CNH_2	C_s	A-pl	−95.200 20 (2)	6.04	1.432	1.091, 1.086 (2)[f]	0.2	113.7, 110.4 (2)
H_3CNH_2[e]	C_s	P-pl	−95.200 31 (1)	5.97	1.431	1.084, 1.089 (2)[f]	0.0	109.0, 112.8 (2)
H_3CNH_2[e]	C_s	S-ec	−95.206 02 (1)	2.39	1.460	1.085, 1.086 (2)[f]	29.5	110.7, 111.8 (2)
H_3CNH_2[e]	C_s	A-st	−95.209 83 (0)	0.00	1.453	1.091, 1.084 (2)[f]	31.8	114.8, 109.2 (2)
FCH_2NH_2	C_s	P-pl	−194.052 66 [2]	12.69	1.419	1.361	0.0	107.3
FCH_2NH_2	C_1	P-st	−194.060 49 [1]	7.77	1.441	1.364	31.9	108.4
FCH_2NH_2	C_s	A-pl	−194.063 94 [1]	5.61	1.397	1.378	3.4	112.6
FCH_2NH_2	C_s	S-ec	−194.064 35 (0)	5.35	1.413	1.371	16.5	111.4
FCH_2NH_2	C_s	A-st	−194.072 88 [0]	0.00	1.412	1.379	28.4	113.1
F_2CHNH_2	C_s	A-pl	−292.930 41 [2]	6.49	1.392	1.342	0.0	109.2
F_2CHNH_2	C_s	P-pl	−292.934 46 [1]	3.95	1.378	1.349	0.0	112.2
F_2CHNH_2	C_s	S-st	−292.935 87 [1]	3.07	1.410	1.337	27.4	108.6
F_2CHNH_2	C_s	A-ec	−292.936 04 [1]	2.96	1.416	1.342	28.8	110.2
F_2CHNH_2	C_1	P-st	−292.940 75 [0]	0.00	1.401	1.334, 1.354	28.4	112.9, 109.2
F_3CNH_2	C_s	A-pl	−391.809 05 [2]	3.78	1.375	1.330, 1.323 (2)	0.4	114.4, 110.8 (2)
F_3CNH_2	C_s	P-pl	−391.809 12 [1]	3.73	1.375	1.320, 1.328 (2)	0.0	109.4, 113.3 (2)
F_3CNH_2	C_s	S-ec	−391.811 68 [1]	2.13	1.397	1.320, 1.325 (2)	23.6	112.7, 111.3 (2)
F_3CNH_2	C_s	A-st	−391.815 07 [0]	0.00	1.394	1.333, 1.317 (2)	27.1	114.1, 110.3 (2)
H_2NNH_2	C_s	A-pl	−111.139 74 (2)	18.59	1.429	1.005[f]	0.2	105.9
H_2NNH_2[e]	C_{2v}	A-ec	−111.152 51 (1)	10.58	1.450	1.002[f]	37.1	108.8
H_2NNH_2[e]	C_s	P-pl	−111.159 54 (1)	6.17	1.381	1.001[f]	0.0[g]	111.3[h]
H_2NNH_2	C_2	*i*	−111.164 86 (1)	2.83	1.449	1.003, 1.003[f]	46.3	105.9, 104.8
H_2NNH_2[e]	C_{2h}	S-st	−111.164 92 (0)	2.79	1.451	1.004[f]	46.6	104.8
H_2NNH_2[e]	C_2	P-st	−111.169 37 (0)	0.00	1.413	1.003, 0.999[f]	41.8	112.2, 107.9
$FNHNH_2$	C_1	P-ec	−209.939 71 (1)	15.93	1.433	1.385	38.7	104.7
$FNHNH_2$	C_1	P-st	−209.949 04 (1)	10.07	1.432	1.380	46.6	103.4
$FNHNH_2$	C_1	A-pl	−209.953 20 (1)	7.46	1.342	1.407	2.4	108.6
$FNHNH_2$	C_1	S-st	−209.954 91 (0)	6.39	1.371	1.390	23.1	107.0
$FNHNH_2$	C_1	A-st	−209.965 09 (0)	0.00	1.369	1.405	30.5	108.4
F_2NNH_2	C_s	A-pl	−308.728 73 [2]	17.08	1.380	1.360	0.0	103.8
F_2NNH_2	C_s	A-ec	−308.742 13 [1]	8.67	1.410	1.360	37.9	105.1
F_2NNH_2	C_s	S-st	−308.746 06 [1]	6.21	1.406	1.350	43.6	103.2
F_2NNH_2	C_s	P-pl	−308.748 20 [1]	4.86	1.326	1.366	0.0	107.7
F_2NNH_2	C_1	P-st	−308.755 95 [0]	0.00	1.363	1.349, 1.372	31.4	107.5, 105.1
$HONH_2$[e]	C_s	P-pl	−130.941 76 (2)	23.27	1.395	0.946[f]	0.0	106.0
$HONH_2$	C_s	A-pl	−130.956 44 (1)	14.06	1.368	0.949[f]	0.1	107.0
$HONH_2$	C_1	P-st	−130.964 95 (1)	8.72	1.415	0.946[f]	43.2	108.2
$HONH_2$[e]	C_s	A-st	−130.969 99 (0)	5.55	1.394	0.950[f]	35.6	109.2
$HONH_2$[e]	C_s	S-st	−130.978 84 (0)	0.00	1.404	0.946[f]	44.0	104.1
$FONH_2$	C_s	P-pl	−229.669 43 [2]	29.01	1.394	1.367	0.0	103.4
$FONH_2$	C_1	P-st	−229.696 32 [1]	12.14	1.416	1.371	49.0	104.6
$FONH_2$	C_s	A-pl	−229.701 39 [1]	8.95	1.305	1.416	1.2	107.9
$FONH_2$	C_s	S-st	−229.708 54 [0]	4.47	1.360	1.381	36.4	105.9
$FONH_2$	C_s	A-st	−229.715 66 [0]	0.00	1.342	1.402	33.1	107.5

[a] Notation for conformations is defined in the text; relative energies E_{rel} of conformers of the same molecule are given in kcal/mol, bond lengths in Å, and angles in degrees. [b] Total energy in au, with the number of imaginary vibrational frequencies given in parentheses if computed and in brackets if assumed (not computed). [c] The degree of pyramidalization at the nitrogen of the NH_2 group is represented by $\Delta\theta$(N), which is 360 minus the sum of the three bond angles at N. [d] For the non-fluorinated species, the values of θ(HAN) are given. [e] From ref 32a. [f] The A–H bond lengths in non-fluorinated species. [g] The value of $\Delta\theta$(N) at the nonplanar nitrogen is 28.3°. [h] This is the value at the nonplanar nitrogen; the values at the planar nitrogen are 122.1 and 117.2°. [i] Transition structure for internal rotation between P-st (C_2; gauche) and S-st (C_{2h}; anti) minima.

through ab initio SCF geometry optimizations on various possible conformations and stationary points. The GAUSSIAN 82 program[30] was employed, including its standard basis sets and methods.[30c] While initial HF/3-21G geometry optimizations were done for some of the species, it is well-known that the smallest basis set level capable of giving reasonable representations of bond angles and inversion barriers in amines is valence-double-ζ plus polarization (see, e.g., ref 30c). Therefore, full geometry optimizations (using gradient techniques) were carried out for all species at HF/6-31G*. (Pyramidalization at N was confirmed in this study to be seriously underestimated by 3-21G.) Some of the more difficult transition structure optimizations were performed with the eigenvector-following algorithm of Baker.[30b] For a few representative species, the influence of electron correlation on energies and geometries was investigated with Møller–Plesset perturbation theory,[30c] as reported in section III-H (full details are given in the supplementary material).

(30) (a) Binkley, J. S.; Frisch, M. J.; DeFrees, D. J.; Raghavachari, K.; Whiteside, R. A.; Schlegel, H. B.; Fluder, E. M.; Pople, J. A. "GAUSSIAN 82 (release H version)"; Carnegie-Mellon University: Pittsburgh, PA, 1983. This program has been modified by A. Sawaryn and T. Kovar for the Cyber 855 computer and by Convex for the Convex C-1 computer. (b) Baker, J. *J. Comput. Chem.* **1986**, *7*, 385–395. (c) Hehre, W. J.; Radom, L.; Schleyer, P. v. R.; Pople, J. A. *Ab initio Molecular Orbital Theory*; Wiley: New York, 1986.

Table II. Summary of HF/6-31G* Geometries and Energies for Second-Row $F_nAH_mNH_2$ Species[a]

	sym	conformn	E[b]	E_{rel}	R(AN)	R(AF)	$\Delta\theta$(N)[c]	θ(FAN)[d]
$HMgNH_2$[e]	C_{2v}	P-pl	−255.777 09 (0)	0.00	1.894	1.715[f]	0.0	180.0
$FMgNH_2$	C_{2v}	P-pl	−354.720 38 [0]	0.00	1.886	1.731	0.0	180.0
H_2AlNH_2[e]	C_{2v}	A-pl	−298.678 25 (1)	11.19	1.794	1.587[f]	0.0	121.3
H_2AlNH_2[e]	C_{2v}	P-pl	−298.696 09 (0)	0.00	1.771	1.583[f]	0.0	118.4
$FAlHNH_2$	C_s	A-st	−397.629 92 [1]	8.31	1.782	1.643	3.0	118.9
$FAlHNH_2$	C_s	P-pl	−397.643 16 [0]	0.00	1.762	1.641	0.0	118.0
F_2AlNH_2	C_{2v}	A-pl	−496.575 38 [1]	7.56	1.765	1.632	0.0	123.2
F_2AlNH_2	C_{2v}	P-pl	−496.587 42 [0]	0.00	1.751	1.631	0.0	121.1
H_3SiNH_2[e]	C_s	P-pl	−346.283 38 (1)	0.35	1.717	1.476, 1.479 (2)[f]	0.0	106.6, 112.9 (2)
H_3SiNH_2[e]	C_s	A-st	−346.283 94 (0)	0.00	1.724	1.482, 1.475 (2)[f]	7.8	115.5, 108.2 (2)
$FSiH_2NH_2$	C_s	P-pl	−445.214 15 (2)	3.58	1.704	1.594	0.0	105.3
$FSiH_2NH_2$	C_1	P-st	−445.214 16 [1]	3.58	1.705	1.594	0.8	105.4
$FSiH_2NH_2$	C_s	A-st	−445.219 86 [0]	0.00	1.702	1.599	4.4	114.0
F_2SiHNH_2	C_s	A-ec	−544.154 73 [1]	0.69	1.689	1.582	0.8	108.4
F_2SiHNH_2	C_s	P-pl	−544.155 83 [0]	0.00	1.686	1.584	0.0	112.0
F_3SiNH_2	C_s	A-st	−643.091 86 [0]	0.00	1.675	1.573, 1.570 (2)	1.0	115.6, 109.7 (2)
H_2PNH_2	C_s	A-pl	−397.465 68 (2)	10.01	1.718	1.409[f]	0.1	98.8
H_2PNH_2[e]	C_s	A-ec	−397.469 24 (1)	7.78	1.747	1.409[f]	24.7	100.1
H_2PNH_2[e]	C_s	S-st	−397.472 43 (1)	5.78	1.752	1.403[f]	32.3	97.3
H_2PNH_2[e]	C_s	P-pl	−397.480 64 (1)	0.63	1.687	1.406[f]	0.0	102.2
H_2PNH_2[e]	C_1	P-st	−397.481 64 (0)	0.00	1.706	1.410, 1.401[f]	13.9	103.7, 99.5
$FPHNH_2$	C_1	P-ec	−496.358 25 (1)	11.68	1.721	1.602	24.2	98.2
$FPHNH_2$	C_1	A-st	−496.376 87 (0)	0.00	1.674	1.608	9.7	104.8
F_2PNH_2	C_s	A-pl	−595.270 03 [2]	7.46	1.673	1.583	0.2	97.4
F_2PNH_2	C_s	S-st	−595.271 20 [1]	6.73	1.689	1.578	18.1	96.7
F_2PNH_2	C_s	A-ec	−595.272 00 [1]	6.22	1.689	1.587	19.3	98.5
F_2PNH_2	C_s	P-pl	−595.281 77 [1]	0.09	1.649	1.586	0.0	100.6
F_2PNH_2	C_1	P-st	−595.281 92 [0]	0.00	1.655	1.582, 1.589	5.6	102.3, 98.6
$HSNH_2$[e]	C_s	P-pl	−453.647 79 (2)	16.35	1.713	1.323[f]	0.0	96.1
$HSNH_2$	C_1	P-st	−453.660 72 (1)	8.23	1.755	1.325[f]	38.9	97.4
$HSNH_2$	C_s	A-pl	−453.670 19 (1)	2.29	1.664	1.334[f]	0.0	101.5
$HSNH_2$[e]	C_s	A-st	−453.673 84 (0)	0.53	1.695	1.334[f]	21.5	102.6
$HSNH_2$	C_s	S-st	−453.674 69 (0)	0.00	1.710	1.326[f]	27.7	97.9
$FSNH_2$	C_s	P-pl	−552.472 58 [2]	27.00	1.698	1.608	0.0	95.1
$FSNH_2$[g]	C_s	A-pl[g]	−552.480 17[g]	22.24	1.692	1.597	0.0	100.8
$FSNH_2$	C_1	P-st	−552.486 50 [1]	18.27	1.733	1.609	41.3	96.2
$FSNH_2$	C_s	A-pl	−552.513 27 [*h*]	1.47	1.615	1.625	0.0	103.8
$FSNH_2$	C_s	A-st	−552.515 61 [0]	0.00	1.631	1.626	11.6	103.9
$ClSNH_2$	C_s	P-pl	−912.537 35 [2]	24.33	1.706	2.023	0.0	98.1
$ClSNH_2$	C_1	P-st	−912.550 72 [1]	15.94	1.746	2.026	40.0	99.5
$ClSNH_2$	C_s	A-pl	−912.573 27 [*h*]	1.79	1.622	2.077	0.0	105.6
$ClSNH_2$	C_s	A-st	−912.576 13 [0]	0.00	1.642	2.074	13.3	105.8

[a] Notation for conformations is defined in the text; relative energies E_{rel} of conformers of the same molecule are given in kcal/mol, bond lengths in Å, and angles in degrees. For the $ClSNH_2$ species, the S–Cl length and NSCl angle are given in the R(AF) and θ(FAN) columns. [b] Total energy in au, with the number of imaginary vibrational frequencies given in parentheses if computed and in brackets if assumed (not computed). [c] The degree of pyramidalization at the nitrogen of the NH_2 group is represented by $\Delta\theta$(N), which is 360 minus the sum of the three bond angles at N. [d] For the non-fluorinated species, the values of θ(HAN) are given. [e] From ref 32a. [f] The A–H bond lengths are given for the non-fluorinated species. [g] Geometry optimization carried out with respect to the *truncated* HF/6-31G* energy where the $n_N \rightarrow \sigma_{SF}^*$ interaction has been zeroed (see text). [h] This species, with a planar SNH_2 unit, is not a stationary point on the potential energy surface (see text, section III-F).

Geometry optimization was carried out with analytic gradients at second order (MP2FU), allowing correlation of all electrons ("full", or "FU"), and energies were evaluated in the frozen core approximation ("FC") to second order (MP2FC) or to full fourth order (MP4SDTQ).[30c] In some cases, the basis set was expanded to include diffuse functions (+) on all heavy atoms (6-31+G*).[30c] The influence of correlation was found to be rather unimportant. For FCH_2NH_2 and $FSNH_2$, comparison calculations with the semiempirical methods MNDO and AM1[31] were performed.

Total HF/6-31G* energies at the HF/6-31G* geometries (denoted as HF/6-31G*//HF/6-31G* level of theory) are given in Tables I and II, along with the major geometrical parameters (the full HF/6-31G* geometries are given as supplementary material). The amount of pyramidalization at the NH_2 nitrogen is quantified by subtracting the sum of the three bond angles at N from 360°; this is denoted as $\Delta\theta$(N) and presented in Tables I and II. It has a value of 38.4° in NH_3 at the HF/6-31G* level[32] and would be 31.59° (360° − 3(109.47°)) for an amino group with tetrahedral angles. Barriers for inversion and internal rotation are obtainable from Tables I and II and are compiled in Tables III and IV. For reference, the HF/6-31G* inversion barrier of NH_3 is 6.51 kcal/mol.[32]

Since there are many possible conformations, transition structures, and other stationary points of the $F_nAH_mNH_2$ species, a shorthand notation is helpful. The dihedral angle relationship between the nitrogen lone pair and the A–F bond in monofluorinated species (n = 1) is designated by A (anti, ≃180°), S (syn, ≃0°), or P (perpendicular, ≃90°). This designation is employed for the structures of F_2BNH_2 and F_2AlNH_2, which are either P (fully planar) or A (90° twisted). For the remaining difluorinated species (n = 2), the dihedral angle between n_N and the

(31) (a) MNDO: Dewar, M. J. S.; Thiel, W. *J. Am. Chem. Soc.* **1977**, *99*, 4899–4906. (b) MNDO fluorine parameters: Dewar, M. J. S.; Rzepa, H. S. *J. Am. Chem. Soc.* **1978**, *100*, 58–67. (c) MNDO sulfur parameters: Dewar, M. J. S.; Reynolds, C. H. *J. Comput. Chem.* **1986**, *7*, 140–143. (d) AM1: Dewar, M. J. S.; Zoebisch, E. G.; Healy, E. F.; Stewart, J. J. P. *J. Am. Chem. Soc.* **1985**, *107*, 3902–3909. (e) AM1 fluorine parameters: Dewar, M. J. S.; Zoebisch, E. G., unpublished results. (f) Baird, N. C. *Can. J. Chem.* **1983**, *61*, 1567–1572.

(32) (a) Whiteside, R. A.; Frisch, M. J.; Pople, J. A. *The Carnegie-Mellon Quantum Chemistry Archive*, 3rd ed.; Carnegie-Mellon University: Pittsburgh, PA, 1983. In the archive, *syn*-$HSNH_2$ is improperly labeled as trans, and it should be cautioned that the planar-SNH_2 structure of $HSNH_2$, though close to the C_s TS stationary point, is not a stationary point on the PES even though its frequencies were computed. (b) In one previous work, the C_s TS (A-pl) structure of $HSNH_2$ was incorrectly indicated as being an energy minimum: Magnusson, E. *J. Comput. Chem.* **1984**, *5*, 612–628.

Table III. Stabilization Energies by Eq 1 and Internal Rotation and Inversion Barriers for First-Row $F_nAH_mNH_2$ Species at the HF/6-31G*//HF/6-31G* Level of Theory (kcal/mol)

			E		
$F_nAH_mNH_2$	sym	conformn	stab.	rot.	inv
$FBeNH_2$	C_{2v}	P-pl	−3.76		
H_2BNH_2	C_s	A-st			4.39
H_2BNH_2	C_{2v}	P-pl		29.44	
$FBHNH_2$	C_s	A-pl	8.23		
$FBHNH_2$	C_s	S-st	6.39		2.56
$FBHNH_2$	C_s	A-st	6.58		2.76
$FBHNH_2$	C_s	P-pl	−1.09	21.76	
F_2BNH_2	C_{2v}	A-pl	8.01		
F_2BNH_2	C_s	A-st	5.80		2.18
F_2BNH_2	C_{2v}	P-pl	−5.34	18.30	
H_3CNH_2	C_s	P-pl		0.07	
H_3CNH_2	C_s	A-st		2.39	5.97
FCH_2NH_2	C_s	P-pl	8.09		
FCH_2NH_2	C_1	P-st	7.03		4.92
FCH_2NH_2	C_s	A-pl	15.17	7.08	
FCH_2NH_2	C_s	S-ec	11.85	2.42	0.26
FCH_2NH_2	C_s	A-st	14.81	7.77	5.61
F_2CHNH_2	C_s	A-pl	18.22		
F_2CHNH_2	C_s	P-pl	20.69	2.54	
F_2CHNH_2	C_s	S-st	15.60		3.42
F_2CHNH_2	C_s	A-ec	18.10		3.53
F_2CHNH_2	C_1	P-st	18.66	2.96	3.95
F_3CNH_2	C_s	A-pl	20.32		
F_3CNH_2	C_s	P-pl	20.29	0.05	
F_3CNH_2	C_s	S-ec	18.05		
F_3CNH_2	C_s	A-st	18.32	2.13	3.73
H_2NNH_2	C_{2v}	A-ec			8.01
H_2NNH_2	C_{2h}	S-st			
H_2NNH_2	C_s	P-pl		12.42	
H_2NNH_2	C_2	P-st		2.83	6.17
$FNHNH_2$	C_1	P-ec	−0.68		
$FNHNH_2$	C_1	P-st	7.97		
$FNHNH_2$	C_1	A-pl	13.96		
$FNHNH_2$	C_1	S-ec	8.86		1.07
$FNHNH_2$	C_1	A-st	15.25	10.07	7.46
F_2NNH_2	C_s	A-pl	18.94		
F_2NNH_2	C_s	A-ec	19.34		8.41
F_2NNH_2	C_s	S-st	14.02		10.87
F_2NNH_2	C_s	P-pl	18.74	13.22	
F_2NNH_2	C_1	P-st	17.43	6.21	4.86
$HONH_2$	C_1	P-st			14.55
$HONH_2$	C_s	A-pl		9.21	
$HONH_2$	C_s	S-st		8.72	14.06
$HONH_2$	C_s	A-st		3.17	8.51
$FONH_2$	C_s	P-pl	5.55		
$FONH_2$	C_1	P-st	7.87		16.87
$FONH_2$	C_s	A-pl	16.39	20.06	
$FONH_2$	C_s	S-st	6.82	7.67	4.48
$FONH_2$	C_s	A-st	16.84	12.14	8.95

bisector of the FAF angle is designated as A, S, or P. In trifluorinated species ($n = 3$), the dihedral angle between n_N and the *unique* A–F bond is designated as A, S, or P. In addition, we denote the configuration of the hydrogens at N with respect to the F_nAH_m group as "st" (staggered), "ec" (eclipsed), or "pl" (planar). For FCH_2NH_2, for instance, the most favorable conformation is A-st, and the transition structure for internal rotation is P-st. This notation is utilized in the tables, where the point-group symmetry is given also. For convenience, schematic diagrams of the various conformations for each molecule are given in the text, as these are discussed in section III. The different stationary points on the potential energy surface of each molecule can be characterized by the number of imaginary vibrational frequencies that they possess, N_{imag}.[30c] The computation of vibrational frequencies is time-consuming, and it was impractical (and unnecessary) to compute these for all of the stationary structures given in Tables I and II. The values of N_{imag} can be guessed reliably in most cases from the energy and geometry data for the different stationary points found for each molecule and are given in brackets after the energies in the tables. This allows one to see at a glance what

Table IV. Stabilization Energies by Eq 1 and Internal Rotation and Inversion Energy Barriers for Second-Row $F_nAH_mNH_2$ Species, HF/6-31G*//HF/6-31G* Level (kcal/mol)[a]

			E		
$F_nAH_mNH_2$	sym	conformn	stab.	rot.	inv
$FMgNH_2$	C_{2v}	P-pl	−1.11		
H_2AlNH_2	C_{2v}	P-pl		11.19	
$FAlHNH_2$	C_s	A-st	2.89		
$FAlHNH_2$	C_s	P-pl	0.00	8.31	
F_2AlNH_2	C_{2v}	A-pl	2.01		
F_2AlNH_2	C_{2v}	P-pl	−1.63	7.56	
H_3SiNH_2	C_s	A-st		0.35	0.35
$FSiH_2NH_2$	C_s	P-pl	4.71		
$FSiH_2NH_2$	C_1	P-st	4.36		0.001
$FSiH_2NH_2$	C_s	A-st	7.94	3.57	
F_2SiHNH_2	C_s	A-ec	9.21		
F_2SiHNH_2	C_s	P-pl	9.54	0.69	
F_3SiNH_2	C_s	A-st	9.24		[<0.01]
H_2PNH_2	C_s	S-st			4.23
H_2PNH_2	C_s	A-ec			2.23
H_2PNH_2	C_s	P-pl		9.38	
H_2PNH_2	C_1	P-st		5.78	0.63
$FPHNH_2$	C_1	P-ec	10.53		
$FPHNH_2$	C_1	A-st	14.43	11.68	
F_2PNH_2	C_s	A-pl	23.56		
F_2PNH_2	C_s	S-st	20.06		0.73
F_2PNH_2	C_s	A-ec	22.56		1.24
F_2PNH_2	C_s	P-pl	21.54	6.37	
F_2PNH_2	C_1	P-st	21.01	6.22	0.09
$HSNH_2$	C_1	P-st			8.12
$HSNH_2$	C_s	A-pl		14.06	
$HSNH_2$	C_s	S-st		8.23	2.29
$HSNH_2$	C_s	A-st		7.73	1.76
$FSNH_2$	C_s	P-pl	8.04		
$FSNH_2$	C_1	P-st	8.66		8.73
$FSNH_2$	C_s	A-pl	19.48	25.53	
$FSNH_2$	C_s	A-st	18.69	18.27	
$ClSNH_2$	C_s	P-pl	4.29		
$ClSNH_2$	C_1	P-st	4.57		8.39
$ClSNH_2$	C_s	A-pl	12.78	22.64	
$ClSNH_2$	C_s	A-st	12.28	15.94	

[a] Value in brackets is estimated.

structures are minima ($N_{imag} = 0$), transition structures (TS; $N_{imag} = 1$), and "transition structures" between transition structures ($N_{imag} = 2$). For some of the potentially doubtful cases of the monofluorinated species, N_{imag} has been computed analytically, and these values are given in parentheses in the tables. In each case where N_{imag} was analytically computed, the presumed value of N_{imag} was confirmed.

Tables III and IV present the net energetic stabilizations according to the isodesmic equation

$$F_nAH_mNH_2 + AH_{n+m+1} \rightarrow F_nAH_{m+1} + H_{m+n}ANH_2 \qquad (1)$$

The necessary HF/6-31G*//HF/6-31G* energies for the reference AH_{n+m+1}, F_nAH_{m+1}, and $H_{m+n}ANH_2$ species were taken primarily from ref 32 and from our previous work.[2c] The energies of the remaining species were computed in this work (the optimized geometries are given in the supplementary material). In all cases, the ΔE values of eq 1 were computed with $F_nAH_mNH_2$ and $H_{m+n}ANH_2$ in analogous conformations. Conformations of the $H_{m+n}ANH_2$ species are defined in the same way as for the corresponding $F_{m+n}ANH_2$ species, the dihedral angles being defined with respect to the unique AH bond or the HAH bisector. The ΔE value by eq 1 for the A-pl structure of F_2NNH_2, for instance, is computed by using the energy of the A-pl structure of H_2NNH_2. The energies and chief geometrical parameters of the $H_{m+n}ANH_2$ species are given in Tables I and II. For all of the $H_{m+n}ANH_2$ species, the analytically computed value of N_{imag} is given, being taken when available from ref 32.

Additionally, we studied the relationship between the anomeric effect and negative hyperconjugation in $FSNH_2$ by analyzing the calculated HF/6-31G* wave functions with the natural bond orbital (NBO) set of methods,[13] using the program G82NBO.[33] (Where appropriate, aspects

Table V. Increments of Stabilization Energy ΔE (Eq 1) and Geometrical Parameters of Monofluorinated Amines Due to Electrostatic (ES) and Negative Hyperconjugation (NH) Effects[a]

species	ref	effect	$\Delta\Delta E$	ΔR(AN)	ΔR(AF)	$\Delta\theta$(FAN)	$\Delta\Delta\theta$(N)
FCH_2NH_2(P-pl)	H_3CNH_2(P-pl)	ES	+8.09	−0.012			
FCH_2NH_2(A-pl)	FCH_2NH_2(P-pl)	NH	+7.08	−0.022	+0.017	+5.3	
FCH_2NH_2(P-st)	H_3CNH_2(P-st)	ES	+7.03	−0.012			+0.1
FCH_2NH_2(A-st)	FCH_2NH_2(P-st)	NH	+7.78	−0.029	+0.015	+4.7	−3.5
$FNHNH_2$(P-ec)	H_2NNH_2(A-ec)	ES	−0.68	−0.017		−4.1	+1.6
$FNHNH_2$(A-st)	$FNHNH_2$(P-ec)	NH	+15.93	−0.064	+0.020	+3.7	−8.2
$FONH_2$(P-pl)	$HONH_2$(P-pl)	ES	+5.55	−0.001		−2.6	
$FONH_2$(A-pl)	$FONH_2$(P-pl)	NH	+10.84	−0.089	+0.049	+4.5	
$FONH_2$(P-st)	$HONH_2$(P-st)	ES	+7.87	+0.001		−3.6	+5.8
$FONH_2$(A-st)	$FONH_2$(P-st)	NH	+8.97	−0.074	+0.031	+2.9	−15.9
$FSiH_2NH_2$(P-pl)	H_3SiNH_2(P-pl)	ES	+4.71	−0.013			
$FSiH_2NH_2$(A-st)	$FSiH_2NH_2$(P-pl)	NH	+3.23	−0.002	+0.005	+8.7	
$FPHNH_2$(P-ec)	H_2PNH_2(A-ec)	ES	+10.43	−0.026		−1.9	−0.5
$FPHNH_2$(A-st)	$FPHNH_2$(P-ec)	NH	+3.90	−0.047	+0.006	+6.6	−14.5
$FSNH_2$(P-pl)	$HSNH_2$(P-pl)	ES	+8.04	−0.015		−1.0	
$FSNH_2$(A-pl)	$FSNH_2$(P-pl)	NH	+11.44	−0.083	+0.017	+8.7	
$FSNH_2$(P-st)	$HSNH_2$(P-st)	ES	+8.66	−0.022		−1.2	+2.4
$FSNH_2$(A-st)	$FSNH_2$(P-st)	NH	+10.30	−0.102	+0.017	+7.7	−29.7
$ClSNH_2$(P-pl)	$HSNH_2$(P-pl)	ES	+4.29	−0.007		+2.0	
$ClSNH_2$(A-pl)	$ClSNH_2$(P-pl)	NH	+8.49	−0.084	+0.054	+7.5	
$ClSNH_2$(P-st)	$HSNH_2$(P-st)	ES	+4.57	−0.009		+2.1	+1.1
$ClSNH_2$(A-st)	$ClSNH_2$(P-st)	NH	+7.71	−0.104	+0.048	+6.3	−26.7

[a] See text, section III-A. Energies are in kcal/mol, distances in Å, and angles in degrees.

of the NBO analysis of the other $F_nAH_mNH_2$ species are discussed also.) The steps of the analysis method involve natural population analysis (NPA),[13b] the formation of the strictly localized natural bond orbitals,[13a] and finally, the formation of natural localized molecular orbitals (NLMOs)[13c] by allowing the natural bond orbitals to delocalize to full occupancy. Quantitative analysis of hyperconjugation interactions between various NBOs was performed by using the NBO Fock matrix deletion procedure.[13d] This is a part of the G82NBO program and is described here briefly. In the deletion procedure, one sets the elements of the NBO Fock matrix to zero that correspond to a specific set of delocalization interactions and then diagonalizes this deleted Fock matrix to form new molecular orbitals and hence a new density matrix. The new (deletion) energy is computed by carrying out a single SCF iteration (in the process of which a new Fock matrix is constructed). (Further SCF iterations would lead eventually to the original SCF energy and density matrix.) The procedure is, strictly speaking, not self-consistent, but as long as the particular interactions in the Fock matrix that have been zeroed are not strongly coupled with other interactions that have *not* been zeroed, the error in the energy obtained is not significant.[13d]

The calculations reported were performed with VAX-11/780, Cyber 855, and Convex C-1 computers.[30]

III. Results and Discussion

A. General Remarks. The species listed in Tables I and II display a large range of relative energies, A–N bond lengths, and degree of pyramidalization at the NH_2 group, $\Delta\theta$(N). Several general trends can be noted: (1) The more fluorines are present, the shorter the A–N bond length, the smaller the values of $\Delta\theta$(N) and of the inversion barriers at N, and the larger the stabilization energies by eq 1. (2) Among different conformers of the same molecule, shorter A–N bonds, longer A–F bonds, and larger FAN angles occur as the n_N–σ_{AF}* dihedral angle becomes more favorable for hyperconjugation (180° is better than 0° is better than 90°) and as the NH_2 group is planarized (compare A-pl with A-st or A-ec and compare P-pl with P-st or P-ec). These trends are consistent with the anomeric effect and the negative hyperconjugation model and are seen to some extent already in the nonfluorinated species (see the A–N and A–H bond lengths and HAN angles in Tables I and II).

The high electronegativity of fluorine can play a direct role in the geometrical changes: Increases in n (number of fluorines) will tend to reduce A–N and A–F bond lengths through charge withdrawal (i.e., reduction of the covalent radii of atoms A and N).[2c] Furthermore, inversion barriers tend to increase with substituent electronegativity, due to the increased p character of the bonds.[34] The highest degree of pyramidalization at N is found in the C_1 transition structure (P-st) of $FONH_2$ (49°), which is the amine with the most electronegative substituent (OF); for comparison, the value in NH_3 is 38°. From these considerations, it is clear that negative hyperconjugation and substituent electronegativity act in concert to shorten A–N bonds but compete with regard to the A–F bond length and the degree of pyramidalization at NH_2. These two influences can be separated roughly from each other by comparing conformations of the monofluorinated species that either facilitate or prohibit the orbital overlap required by negative hyperconjugation.[2a,27]

Such comparisons are presented in Table V (species of B and Al are left out due to the complicating factor of π_{AN} bonding in their P-pl structures). Comparisons between respective "P" (P-pl or P-st) conformations of monofluorinated and nonfluorinated amines provide estimates of the magnitude of electrostatic effects (though other interactions, such as $\sigma_{NH}\rightarrow\sigma_{AF}$* hyperconjugation,[14] can play a role), whereas comparisons of respective "A" and "P" conformers of the same monofluoro species yield estimates of the *net* influence of $n_N\rightarrow\sigma_{AF}$* hyperconjugation. In Table V, A–N bond length shortenings due to electrostatic effects are on the order of 0.01–0.02 Å (though no shortening is seen in $FONH_2$), whereas AN shortenings due to $n_N\rightarrow\sigma_{AF}$* interaction range from 0.02 to 0.10 Å (with the exception of $FSiH_2NH_2$). The A–F bond lengthenings in Table V range from 0.005 ($FSiH_2NH_2$) to 0.05 Å (A-pl $FONH_2$). Except in the case A = O in Table V, the A–F bonds are quite strong and show relatively little lengthening due to hyperconjugation. In $FONH_2$, the σ_{OF} orbitals are low-lying, which acts to increase $n_N\rightarrow\sigma_{AF}$* interaction. Additionally, due to their weakness, OF bonds will lengthen more per given σ_{AF}* occupancy than other A–F bonds. As a result of $n_N\rightarrow\sigma_{AF}$* interaction (and perhaps also of n_N–σ_{AF} repulsion; see section III-G6), increases in θ(FAN) of 3–9° occur in Table V. It is also

(33) Reed, A. E.; Weinhold, F. *QCPE Bull.* **1985**, *5*, 141–142.

(34) (a) Mislow, K. *Trans. N. Y. Acad. Sci.* **1973**, *35*, 227–242. See also: Androse, J. D.; Rauk, A.; Mislow, K. *J. Am. Chem. Soc.* **1974**, *96*, 6904–6906. (b) Schmiedekamp, A.; Skaarup, S.; Pulay, P.; Boggs, J. E. *J. Chem. Phys.* **1977**, *66*, 5769–5776. See also the discussion of the $X–PH_2$ barrier in ref 35a. (c) Concerning the effect of fluorination on central atom hybridization, see ref 2c.

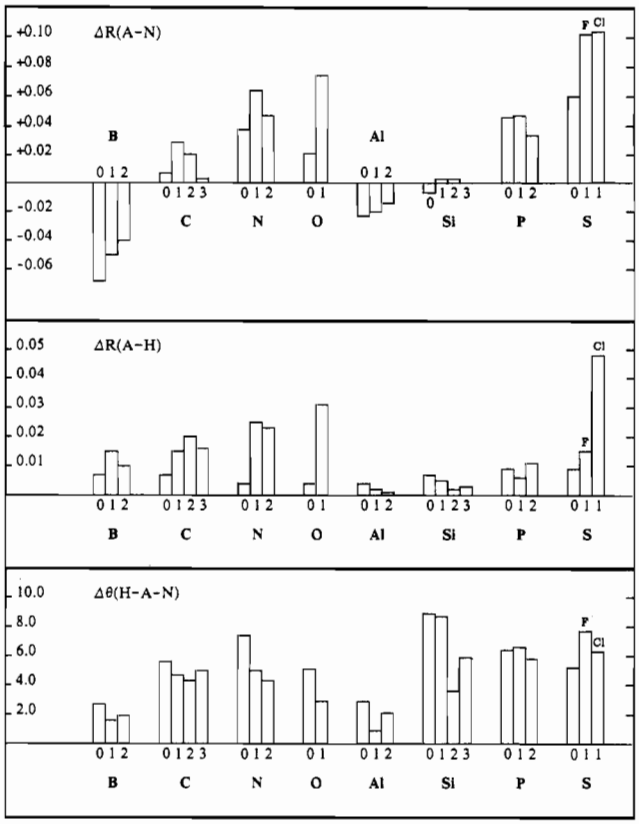

Figure 1. Variation of key HF/6-31G* geometrical parameters (in Å or degrees) with respect to internal rotation in $F_nAH_mNH_2$ species (numbers 0–3 refer to n, the number of fluorines). The value of ΔR(AN) is set to be negative for the B and Al species, where the conformer with the best $n\rightarrow\sigma_{AF}^*$ interaction does not have the shortest value of R(AN). For the $n = 0$ species, values for ΔR(AH) and $\Delta\theta$(HAN) are given; for $ClSNH_2$, ΔR(ACl) and $\Delta\theta$(ClAN) are given.

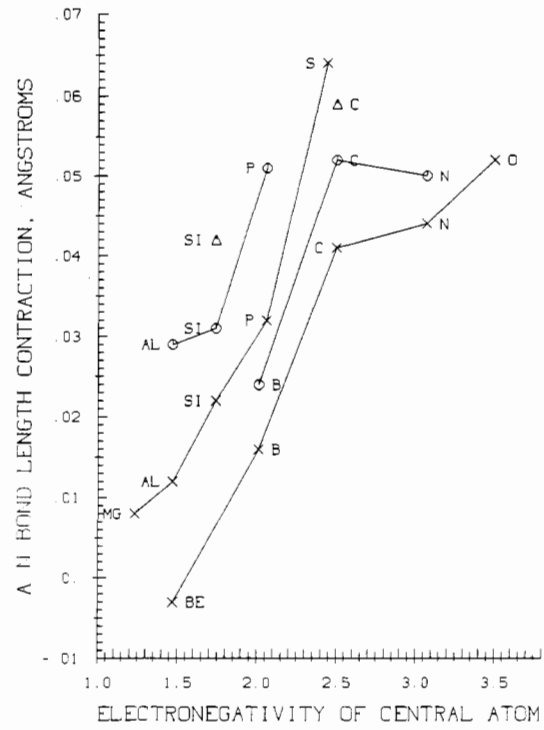

Figure 2. Contraction of the A–N bond (in Å) on going from $AH_{m+n}NH_2$ to $FAH_{m+n-1}NH_2$ (×) to $F_2AH_{m+n-2}NH_2$ (○) and to $F_3AH_{m+n-3}NH_2$ (△), from HF/6-31G* geometries of lowest energy structures, plotted against the Allred–Rochow electronegativity of central atom A. For the B and Al species, the twisted (A-st) conformers are compared.

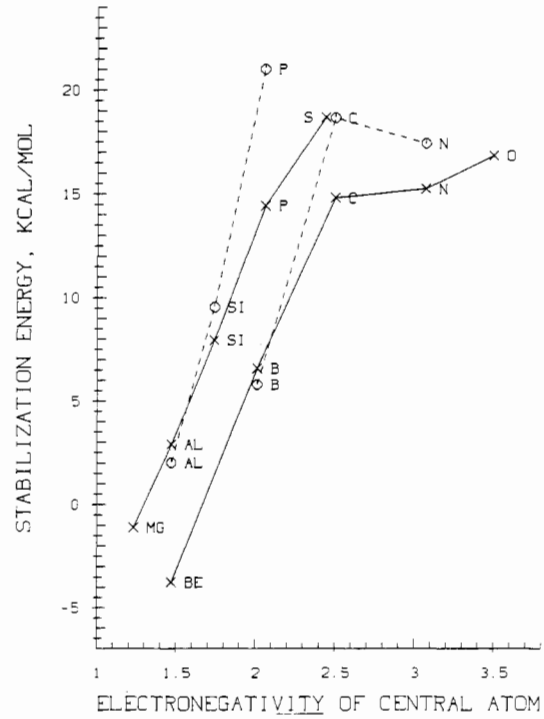

Figure 3. Stabilization energies from eq 1 in kcal/mol for mono- and difluorinated amine species $F_nAH_mNH_2$, plotted against the Allred–Rochow electronegativity of central atom A. For each row, the points for the monofluoro species (×) are connected by full lines and the points for the difluoro species (○) by dotted lines. For the B and Al species, the twisted (A-st) conformers are considered.

apparent that electrostatic and $n_N\rightarrow\sigma_{AF}^*$ hyperconjugative influences on $\Delta\theta$(N) in $FONH_2$ and $FSNH_2$ are opposite in sign. From Table V, the decomposition of the stabilization energies (eq 1) into non-($n_N\rightarrow\sigma_{AF}^*$) and $n_N\rightarrow\sigma_{AF}^*$ origins can be seen. In A-st FCH_2NH_2, for instance, about half of the stabilization energy is due to $n_N\rightarrow\sigma_{AF}^*$, whereas the corresponding figure for $FONH_2$ is two-thirds and, in $FSiH_2NH_2$, less than half. The decomposition of the energy stabilization of $FPHNH_2$ in Table V is somewhat misleading since the P-ec conformer of $FPHNH_2$ is only roughly analogous to the A-ec conformer of H_2PNH_2.

Visualization of the geometric trends in Tables I and II is further aided by Figures 1 and 2. In Figure 1, the difference between the maximum and minimum values of R(AN), R(AF), and θ(FAN) that occur during internal rotation (without inversion) is presented in the form of bar graphs for all species. For the nonfluorinated species ($n = 0$), the variations in R(AH) and θ(HAN) are given. Consistent with negative hyperconjugation, the variation in R(AN) is largest in the monofluorinated species ($n = 1$). In the polyfluorinated species ($n = 2, 3$), the A–F bonds and FAN bond angles are inequivalent within the same structure due to differing n_N–AF dihedral angles (see Tables I and II), and their maximum and minimum values over the conformational surface sometimes occur within the same structure. For example, the maximum and minimum C–F bond lengths in F_2CHNH_2 occur in the lowest energy structure P-st (1.334 and 1.354 Å, from Table I). Although the influence of electrostatic effects on the trends in Figure 1 is negligible, both electrostatic and hyperconjugation effects are responsible for the trends in Figure 2, where the A–N bond lengths in the lowest energy species of each fluoroamine is compared with that of the respective nonfluorinated amine. It is evident from Figure 2 that the more electronegative the central atom A, the greater the A–N bond length contraction due to fluorination. Such a trend was also seen in an analogous plot (Figure 2) in our study of the A–F bond length contraction in the polyfluorinated hydrides.[2c]

The variation of stabilization energy with central atom electronegativity of the mono- and difluorinated amines is shown in Figure 3. Except for the species of B and Al, the stabilization energies plotted are those for the lowest energy conformations of

each molecule, the values being taken from Tables III and IV. For B and Al, the stabilization energies of the twisted (A-st and A-pl, respectively) species were used, since n_N hyperconjugation occurs in these species and not in the planar structures (see below). Along each row of the periodic table, a smooth variation is seen, and the slopes of the respective first- and second-row curves are similar. The second-row curves are displaced to higher energies with respect to the first-row curves, by 5 and 10 kcal/mol for mono- and difluoro species, respectively. The first-row curves level off at higher electronegativities than for carbon due to the decreased polarity of the σ_{AF}* orbital toward atom A. The weakness of N–F and O–F bonds and consequent low energy level of their corresponding antibonds contribute to the strength of stabilization at N and O in Figure 3. This figure should be compared with Figure 3 of ref 2c concerning the polyfluorinated hydrides. Though the stabilization energy curves peak at around carbon in the present study rather than at phosphorus as in the study of the polyfluorides,[2c] the trends are analogous. The variation of negative hyperconjugation with central atom electronegativity has been discussed in detail in the previous work.[2c]

B. Be and Mg Compounds. The stabilization energies ΔE from eq 1 are negative for A = Be, Mg (i.e., destabilizing). Due to the 180° FAN angle, no hyperconjugation can take place. As was found earlier[2c] for F_2Be and F_2Mg, polysubstitution at these centers is unfavorable due to the attenuation of the π-bonding (i.e., two π-donors have less than twice the bonding power as a single π-donor if only one π-acceptor is present). This effect is more pronounced at Be than at Mg due to its greater ability to participate in π-bonding with nitrogen.

C. B and Al Compounds. The two basic conformations of these molecules are planar (P-pl) and 90° twisted (A-pl):

P-pl A-pl

The P-pl species are much lower in energy than the A-pl species because delocalization of the nitrogen lone pair into the formally empty p orbital on B or Al is much more favorable than into B–X antibonds, on both orbital energy and orbital overlap grounds. Pyramidalization at nitrogen is favorable only in the case of the twisted (A-pl) structure of the boron species, resulting in the conformers

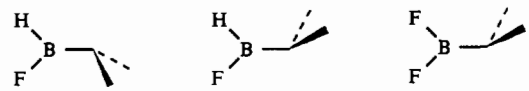

A-st S-st A-st

The A-st conformation of $FAlHNH_2$ is nearly planar, and no S-st or A-pl structures are possible. Optimization of a pyramidal A-st species of C_s symmetry for F_2AlNH_2 results in a structure that is nearly planar and which has an energy identical with that of A-pl; the A-pl structure of F_2AlNH_2 is thus a minimum.

Weak stabilizations (2–8 kcal/mol) are found in the twisted A-pl conformers of the B and Al species, where the trigonal bond angles and the nitrogen lone-pair orientation are favorable for the operation of the anomeric effect. Due to the predominant ionic character of B–F and Al–F bonds, anomeric stabilization energies at B and Al are weak in comparison to those at C centers.[2c] Destabilizations at B and Al are found in the lower energy planar conformations of P-pl type. Here, n_N donates into the formally empty p orbital on B or Al, and π-attenuation occurs, as we have discussed in the case of the polyfluorides.[2c] The inversion barrier at N in the A-st species is progressively reduced by fluorination, from 4.4 (H_2BNH_2) to 2.8 ($FBHNH_2$) to 2.2 kcal/mol (F_2BNH_2), as is the degree of pyramidalization. A progressive decrease of the rotation barrier of the B and Al species with fluorine substitution is seen also in Tables III and IV. The A–N bond length difference between the planar (P-pl) and twisted (A-pl) conformers also decreases with fluorine substitution (see Figure 1). The values of θ(FAN) are consistently 1–2° greater in A-st and A-pl than in P-pl and S-st structures (Tables I and II). All these trends are consistent with negative hyperconjugation.

For F_2BNH_2, good agreement with the experimentally determined structure[18] is obtained (the HF/6-31G* values are in parentheses; R values are in Å and θ values in deg): R(BN), 1.402 ± 0.024 (1.392); R(BF), 1.325 ± 0.012 (1.320); R(NH), 1.003 ± 0.002 (0.994); θ(FBN), 121.1 (121.2); θ(BNH), 121.5 (122.5). A similar geometry for F_2BNH_2 was calculated by Ha,[19c] who used a 4-31G* basis set. It was noted[18] that the B–F bond length in F_2BNH_2 is 0.014 Å longer than that found in F_2BH, and this is consistent with a π-attenuation effect. The planar $F_nH_mBNH_2$ species are of interest with regard to their B=N double-bond character.[19] A progressive decrease of the polarization of the B–N π-bond toward B with greater fluorine substitution is seen in the NBO analysis, from 12% (H_2BNH_2) to 10% ($FBHNH_2$) to 9% (F_2BNH_2), consistent with previous discussions of π-attenuation in these species.[19b,d] By contrast, the B–N σ-bonds are 23% polarized toward B in all three of these species.

D. C and Si Compounds. For H_3ANH_2 and F_3ANH_2, the possible species are

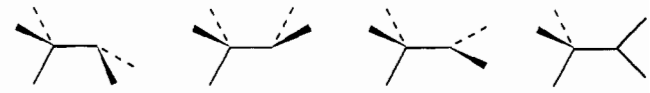

A-st S-ec A-pl P-pl

The five possibilities investigated for FAH_2NH_2 are

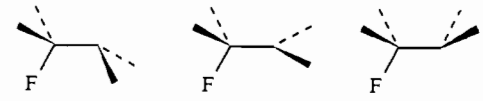

A-st A-pl S-ec

P-pl P-st

Five F_2AHNH_2 species also were studied:

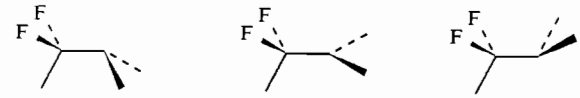

S-st A-pl A-ec

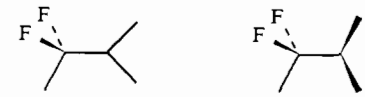

P-pl P-st

Maximum stabilizations by eq 1 for minima are found to be 14.8 (FCH_2NH_2), 18.7 (F_2CHNH_2), 18.3 (F_3CNH_2), 7.9 ($FSiH_2NH_2$), 9.5 (F_2SiHNH_2), and 9.2 kcal/mol (F_3SiNH_2). (As seen in Tables III and IV, stabilizations for some of the inversion transition structures are even greater.) As in the polyfluorinated hydrides,[2c] much greater stabilization is found at C than at Si; this is due to the more favorable (intermediate) electronegativity of carbon for the operation of the anomeric effect.[2c] These results show that only a small increase in stabilization energy occurs on going from n = 1 to n = 2 and no change at all from n = 2 to n = 3. This is in accord with the negative hyperconjugation model: n_N can delocalize into at most two (and not three) σ_{AF}* orbitals. When n_N interacts with two σ_{AF}* orbitals, these are at dihedral angles of ±120° (or 180 and 60°) and thus of much reduced

average *individual* strength compared to interaction with a single σ_{AF}^* orbital at 180°.

The C–N bond lengths in Table I range from 1.460 Å in S-ec H_3CNH_2 to 1.375 Å in A-pl F_3CNH_2, "pl" structures having C–N bonds that are around 0.02 Å shorter than those in the corresponding pyramidal structures. The θ(FCN) values are also interesting. In FCH_2NH_2, for instance, θ(FCN) is 107–108° in P-pl and P-st (hyperconjugation into σ_{CF}^* shut off) and 113° in A-st and A-pl (where this interaction is turned on). (This effect is even stronger in $FSiH_2NH_2$: 105 vs. 114°.)

An interesting finding is that the A-ec (eclipsed) conformation of F_2CHNH_2 is 0.11 kcal/mol *more stable* than S-st, whereas at the same level of theory, staggered H_3CNH_2 is favored by 2.4 kcal/mol over the eclipsed structure. The reversal of ec/st stability can be attributed directly to negative hyperconjugation: In the S-st conformer, the $n_N \rightarrow \sigma_{CF}^*$ dihedral angles are unfavorable (±60°) compared to those in the A-ec conformer (±120°); as a consequence, the stabilization (eq 1) is 2.5 kcal/mol greater in the A-ec conformer (Table III).

With the substitution of a single fluorine, the internal rotation barrier increases significantly, from 2.4 to 7.8 kcal/mol. Further fluorine substitution acts to diminish the rotation barrier to 3.0 (F_2CHNH_2) and 2.1 kcal/mol (F_3CNH_2). The inversion barriers in Table III decrease steadily with fluorine substitution, in spite of the increase in substituent electronegativity: 6.0 (H_3CNH_2) to 5.6 (FCH_2NH_2) to 4.0 (F_2CHNH_2) to 3.7 kcal/mol (F_3CNH_2). The influence of fluorine substitution on the $\Delta\theta$(N) values of these species, however, is smaller, these being 31.8, 28.4, 28.4, and 27.1°, respectively. The earlier calculations of Heaton and Mills[24a] on F_3CNH_2 employed a basis set without polarization functions on carbon and nitrogen. Consequently, the value of $\Delta\theta$(N) was severely underestimated, at 4.0°, in contrast to our value of 27.1°. This illustrates the danger of using sp basis sets for amines. Interestingly, these exists experimental evidence for a significantly nonplanar nitrogen in F_3CNH_2: On the basis of the splitting of the two sharp NH_2 vibrational bands in its IR spectrum, Klöter et al.[23a] estimated an HNH angle of 110.0°. This estimate compares favorably with the HF/6-31G* value of 110.4° obtained in this work.

Heaton and Mills concluded from their calculations on F_3CNH_2 that negative hyperconjugation is not important.[24a] This conclusion was based on the finding that the HOMO of F_3CNH_2 is *more* localized than that of H_3CNH_2. This type of argument is misleading. Though the HOMO in both of these molecules does have its largest contribution from the nitrogen lone pair, significant mixing occurs with lower energy orbitals that have the appropriate symmetry. This latter mixing causes the HOMO to delocalize *independently* of any hyperconjugation interactions, and the amount of this mixing can vary with substitution. In order to compare the amount of hyperconjugative delocalization in two different molecules, it is therefore necessary to analyze them in terms of *localized* orbitals, as is possible through the NBO method (analysis of localized molecular orbitals would also be valid). Indeed, NBO analysis of F_3CNH_2 clearly shows the importance of negative hyperconjugation (we give values for the staggered conformer): The occupancy of the nitrogen lone pair NBO (1.932) is significantly depleted with respect to the ideal value of 2 and with respect to its value in H_3CNH_2 (1.973), and the occupancy of the σ_{CF}^* orbital anti to n_N (0.110) is significantly greater than that in the corresponding molecule F_3CH (0.066). The second-order perturbative estimate[13d] of the anti $n_N \rightarrow \sigma_{CF}^*$ interaction is 25 kcal/mol.

In agreement with Heaton and Mills,[24a] we find no evidence that the low basicity of F_3CNH_2 relative to that of H_3CNH_2 is due to an inductive effect of the fluorines, as suggested earlier.[23] By natural population analysis,[13b] the negative charge on nitrogen gradually *increases* in magnitude with fluorine substitution of methylamine: −0.91 (H_3CNH_2), −0.93 (FCH_2NH_2), −0.95 (F_2CHNH_2), −0.96 (F_3CNH_2). As found previously,[24a] the N–H bonds become more polar toward N with substitution and nitrogen therefore becomes more negatively charged. The *total* charge of the NH_2 group does nevertheless become somewhat less negative with substitution, decreasing from −0.172 to −0.153 on going from H_3CNH_2 to F_3CNH_2. From our above discussion of hyperconjugation in F_3CNH_2, the decreased basicity of this compound relative to that of H_3CNH_2 is understandable in terms of the increased hyperconjugative depletion of the nitrogen lone pair.

The decomposition of F_3CNH_2 by loss of two molecules of HF occurs readily in the gas phase[23] to form FC≡N. This decomposition seems to be driven, however, by entropy, as the reaction energy for the loss of 2 HF from F_3CNH_2 is endothermic at the SCF level of theory (+45 kcal/mol by double-ζ[24a] and +70 kcal/mol by 6-31G*). It would be interesting to test the effect of correlation on the ΔE value for this reaction.

All structures for Si species in Table II are nearly planar at nitrogen, except for staggered SiH_3NH_2, which itself has an inversion barrier of only 0.35 kcal/mol and no minimum for the eclipsed conformer (see also ref 35). The lowest energy structure of $FSiH_2NH_2$(A-st) has a $\Delta\theta$(N) value of only 4.4°, and for this reason, attempts to find a minimum for S-ec or a transition structure for A-pl (analogous to those found for FCH_2NH_2) failed. The transition structure for internal rotation of $FSiH_2NH_2$ has an "inversion barrier" of 0.001 kcal/mol (P-st to P-pl). In the case of F_2SiHNH_2, optimization of a P-st structure of C_1 symmetry led to a nearly planar structure with the same energy as that of P-pl; the P-pl structure is thus a minimum. Only one other stationary point could be found for F_2SiHNH_2, the rotation transition structure A-ec. Since this A-ec structure is almost planar at N, no stationary point could be found for the corresponding staggered species, S-st. (As in F_2CHNH_2, eclipsed A-ec is favored over staggered S-st.) In contrast to the C species, where n_N was found to be significantly depleted as a result of fluorine substitution, little *additional* depletion of n_N was found in the Si species: The occupancy of the n_N NRO decreases from 1.939 in SiH_3NH_2 to 1.931 in F_3SiNH_2. The NBO analysis shows only a small energetic advantage of $n_N \rightarrow \sigma_{SiF}^*$ over $n_N \rightarrow \sigma_{SiH}^*$ interactions. As found in our previous study,[2c] hyperconjugation into Si–F antibonds is weaker than that into C–F bonds due to the much higher ionic character of Si–F bonds. Indeed, the NBOs for the Si–F bonds in F_3SiNH_2 are 88% polarized toward F. As a result, the Si–N distances vary over a smaller range (1.724–1.675 Å) than the C–N distances in Tables I and II.

E. N and P Compounds. We considered five possibilities for H_2ANH_2 and F_2ANH_2 (A = N, P):

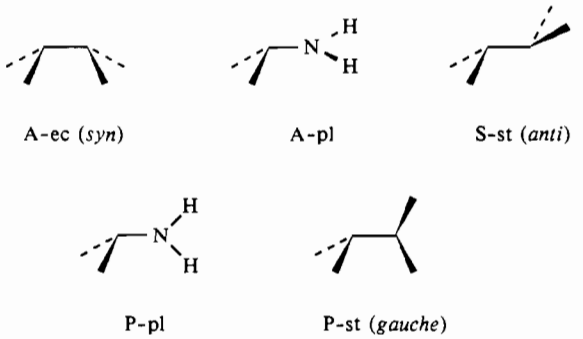

The near-perpendicular (gauche) arrangement of the lone pairs of N and P in the P-st conformations of H_2ANH_2 and F_2ANH_2 is confirmed in the projections along the A–N bond axis of the optimized structures for these species in Figure 4. The potential energy surfaces for $FNHNH_2$ and $FPHNH_2$ are more complicated, as these species have no symmetry. We therefore give projections along the A–N bond axis for all of the optimized

(35) (a) Luke, B. T.; Pople, J. A.; Krogh-Jespersen, M.-B.; Apeloig, Y.; Chandrasekhar, J.; Schleyer, P. v. R. *J. Am. Chem. Soc.* **1986**, *108*, 260–269. (b) Gordon, M. S. *Chem. Phys. Lett.* **1986**, *126*, 451–454. In contrast with the latter work, we have established that no stationary point of H_3SiNH_2 of A-pl type with two imaginary frequencies exists. Also, the HF/6-31G* energies of the latter work differ slightly due to the fact that an earlier version of the 6-31G* basis set for Si had been employed. (c) Experimentally, the $\Delta\theta$(N) value in $H_3SiN(CH_3)_2$ is found to be 5.4 ± 0.7°: Gundersen, G.; Mayo, R. A.; Rankin, D. W. H. *Acta Chem. Scand. Ser., A* **1984**, *38*, 579–591.

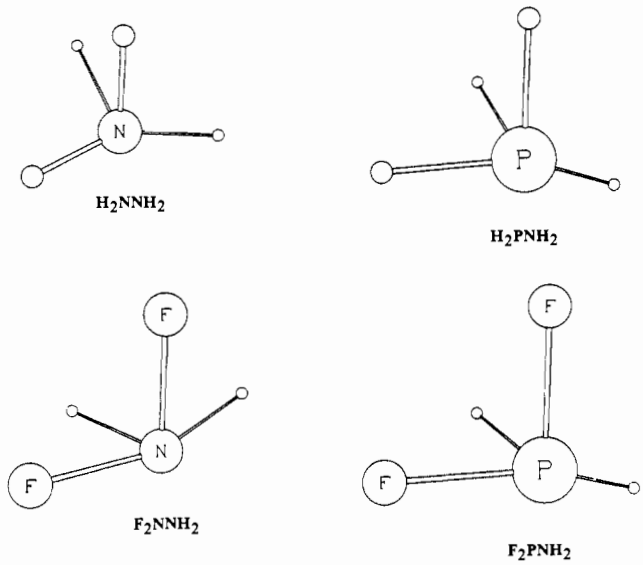

Figure 4. Projections along the A–N axis of the HF/6-31G* optimized geometries of the gauche (P-st) conformations of X_2ANH_2 species (X = H, F; A = N, P).

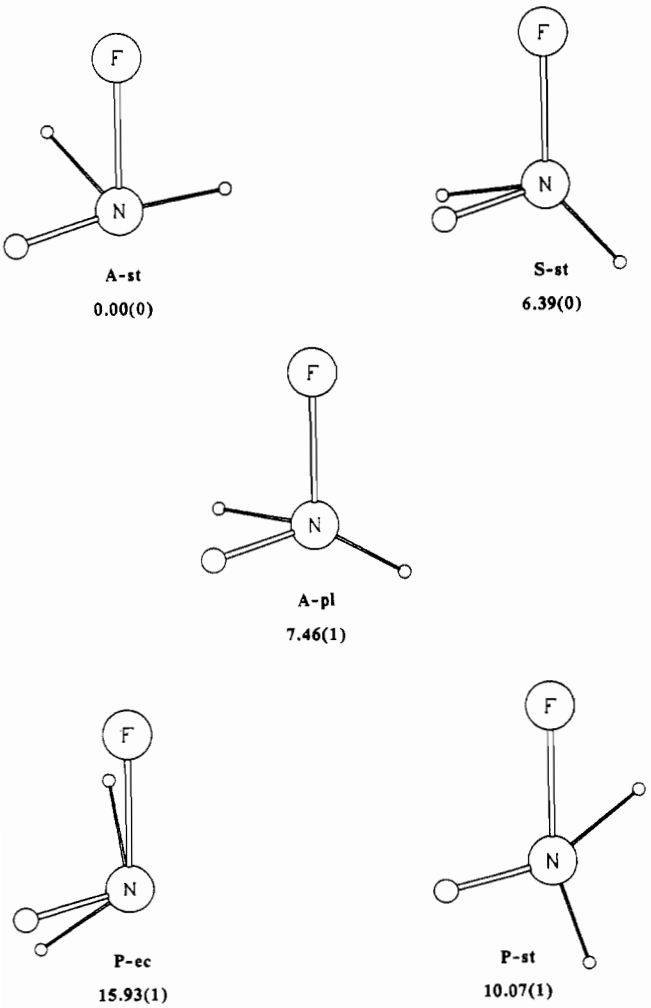

Figure 5. Projections along the N–N axis of the HF/6-31G* optimized geometries of all stationary points of $FNHNH_2$ from Table I, with relative energies given in kcal/mol followed by the number of imaginary frequencies in parentheses.

structures of $FNHNH_2$ and $FPHNH_2$ from Tables I and II, in Figures 5 and 6.

As shown earlier,[25] $FNHNH_2$ has two minimum energy conformers, the nitrogen lone pair of NH_2 being roughly either syn (S-st) or anti (A-st) with respect to the N–F bond. A clear-cut

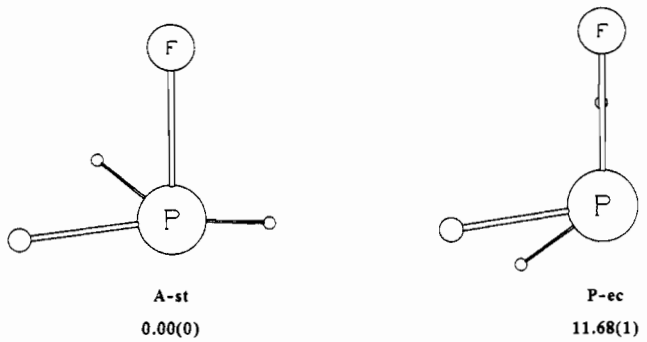

Figure 6. Projections along the P–N axis of the HF/6-31G* optimized geometries of the stationary points of $FPHNH_2$ from Table II, with relative energies given in kcal/mol followed by the number of imaginary frequencies in parentheses.

transition structure (A-pl) for inversion between these two forms was found; this TS is only slightly higher in energy than S-st (7.5 vs 6.4 kcal/mol, relative to A-st). There are two transition structures for internal rotation between the A-st and S-ec minimum structures, one that has the FNH and NH_2 groups approximately eclipsed (analogous to the syn conformer of H_2NNH_2) and is designated P-ec, and another that has the FNH and NH_2 groups staggered (analogous to the anti conformer of H_2NNH_2) and is designated P-st. The barrier to P-ec is 15.9 kcal/mol, and that to P-st is 10.1 kcal/mol (P-st is lower in energy due to stronger $\sigma \rightarrow \sigma^*$ interaction,[14] as verified by NBO analysis of our HF/6-31G* wave functions). Due to lower substituent electronegativity and increased hyperconjugation, the inversion barrier in $FPHNH_2$ should be substantially smaller: the value of $\Delta\theta(N)$ in the A-st conformer of $FPHNH_2$ is only 9.7°, much less than the value of 30.5° in A-st $FNHNH_2$ (see also Figures 5 and 6). It is also less than the value of 11.6° in A-st (syn) $FSNH_2$. Since the latter species is close enough to planarity at N that no inversion can occur (as discussed below), it would not be surprising if no transition structure for inversion and no S-st conformer (with a syn orientation of n_N with respect to the P–F bond) of $FPHNH_2$ exist. Indeed, despite extensive searches with the EF algorithm,[30b] neither could be found. Thus, in contrast to the case for $FNHNH_2$, $FPHNH_2$ has a single minimum (A-st) and a single transition structure for internal rotation (P-ec). As one goes from the A-st to the P-ec structures of $FPHNH_2$, the energy rises by 11.7 kcal/mol (rotation barrier), the P–N bond lengthens by 0.047 Å, the P–F bond shortens by 0.006 Å, the amount of pyramidalization $\Delta\theta(N)$ increases from 9.7 to 24.2°, and the FPN angle decreases by 6.6°, all in line with strong $n_N \rightarrow \sigma_{PF}^*$ hyperconjugation.

Just as in the carbon species, large stabilization energies are found with A = N, P. Difluorination at P results in a larger increase in ΔE than does difluorination at N. The lowest energy conformers of the $n = 2$ species of N and P have C_1 symmetry (P-st). In contrast to the C_1 conformer of F_2NNH_2, the C_1 conformer of F_2PNH_2 is nearly planar at NH_2. The inversion barrier of P-st F_2PNH_2 is only 0.1 kcal/mol, and even in P-st H_2PNH_2 it is only 0.6 kcal/mol. (Accordingly, only a very small planarization energy at N would be expected in $FPHNH_2$, and due to the absence of symmetry in $FPHNH_2$, no stationary point for inversion exists, as discussed above.) This compares with inversion barriers of 4.9 and 6.2 kcal/mol in F_2NNH_2 and H_2NNH_2. The range of N–N bond lengths is impressive, from 1.451 Å in anti H_2NNH_2 to 1.326 Å in P-pl F_2NNH_2, and P–N bond lengths range from 1.752 (anti H_2PNH_2) to 1.649 Å (P-pl F_2PNH_2). Variations in N–F and P–F bond lengths are much smaller but also show consistency. Most dramatically, the two N–F distances in the P-st (C_1) structure of F_2NNH_2 differ by 0.023 Å, the shorter N–F bond being the one that is closest to being anti to the nitrogen lone pair. The θ(FAN) values also vary in a regular manner: In F_2NNH_2, for instance, the largest value of θ(FAN) is 107.7° in P-pl (where the strongest hyperconjugation occurs), and this decreases to 105.1° in A-ec and 103.2° in S-st,

Table VI. Comparison of Geometrical Parameters and Dipole Moment of F_2PNH_2 Obtained by Experiment (Microwave Spectroscopy[21]) and by Theory (HF/6-31G* Optimization)[a]

	exptl	P-pl	P-st
PN	1.650 ± 0.004	1.649	1.655
PF	1.587 ± 0.004	1.586	1.589, 1.582
NH_{cis}	1.002 ± 0.005	0.999	1.000
NH_{trans}	0.981 ± 0.005	0.995	0.997
FPN	100.6 ± 0.2	100.7	102.3, 98.6
PNH_{cis}	123.1 ± 0.2	124.1	121.7
PNH_{trans}	119.7 ± 0.4	120.0	118.3
HNH	117.2 ± 0.4	115.9	114.3
μ	2.58 ± 0.01	2.89	2.75

[a] The theoretical structures given are P-pl, the transition structure for inversion at N (barrier 0.09 kcal/mol), and P-st, the minimum structure. Bond lengths are in Å, angles in degrees, dipole moments in debye.

as hyperconjugation into the N–F antibonds is progressively reduced. In P-st (C_1) F_2NNH_2, the angles are 107.5 and 105.1°, the larger value corresponding to the *longer* N–F bond mentioned above.

An interesting feature in the X_2ANH_2 species is the competition between syn and anti conformers. In H_2NNH_2, anti is 7.8 kcal/mol lower than syn, and N_{imag} for anti is zero. (We have optimized the transition structure of C_2 symmetry for internal rotation between the anti (S-st) and gauche (P-st) minima of H_2NNH_2; this has an energy only 0.04 kcal/mol higher than that of the anti form (Table I). Hence, the anti minimum is very shallow and may not exist at higher levels of theory.) In all other cases, N_{imag} is equal to 1 for both syn and anti forms. In F_2NNH_2, the syn–anti energy difference is reduced to 2.5 kcal/mol and in H_2PNH_2 to 2.0 kcal/mol. Finally, in F_2PNH_2, the preference is reversed, cis being 0.5 kcal/mol lower. Clearly, hyperconjugation acts to favor syn (A-ec) over anti (S-st) conformers and works against the factor of N–N and P–N lone pair–lone pair repulsion that destabilizes the syn orientation.

As shown in Table VI, the calculated HF/6-31G* structural parameters (P-pl structure) of F_2PNH_2 agree rather closely with those determined by microwave spectroscopy[21] (the experimental values have not been corrected for zero-point vibrational motion). The inversion barrier of 0.09 kcal/mol calculated for F_2PNH_2 is certainly less than the zero-point energy associated with out-of-plane bending of the amino group, and the nonplanar structure P-st has a pyramidalization of only 6° at N (see also Figure 4). The potential energy surface for out-of-plane bending at N is thus very soft and hence rather basis-set-sensitive, as was found by Boggs and Niu.[22] The largest basis set employed for F_2PNH_2 in their study was rather imbalanced (with a relatively small sp basis set (4-21G) plus *one* set of d functions on P but *two* sets on N) and led not surprisingly to significantly greater pyramidalization at N due to overemphasis of d functions on N in the basis set. An electron diffraction study[36a] also led to a substantially pyramidal configuration at N, but this result can be disregarded[21] because it was based on a model where the two N–H bonds and the two PNH angles were assumed to be equal. As seen from the microwave and HF/6-31G* structures in Table VI, this assumption is particularly bad in the case of the two PNH angles, which differ by 3–4°.

The P–N bond length in F_2PNH_2 of 1.65 Å is much shorter than that expected on the basis of the Schomaker–Stevenson relation[37] (1.76 Å), even when hybridization changes are taken into account (1.74 Å).[36a] Since, at the 6-31G* level, the P–N double bond in HP=NH has a length of 1.554 Å,[38] the P–N bond length in F_2PNH_2 is roughly halfway between that expected for P–N single and double bonds (the P–N geometric bond order is thus 1.5).[36b] Brittain et al.[21] rationalized the shortness of the P–N bond in terms of p_N–d_P bonding involving a π-type d orbital on P. This hypothesis can be tested directly through NBO analysis. By examining the natural localized molecular orbital[13c] for n_N, we find that the nitrogen lone pair donates 0.096e into the antisymmetric combination of the σ_{PF}* orbitals, 0.075e of this going into a p orbital on P, 0.009e into a d orbital on P, and the remaining 0.012e into orbitals on the two F atoms. Thus, p_N–p_P bonding through negative hyperconjugation (0.075e) is roughly 1 order of magnitude more important than p_N–d_P bonding (0.009e) in F_2PNH_2.

F. O and S Compounds. The possibilities for $XANH_2$ (X = H, F; A = O, S) are

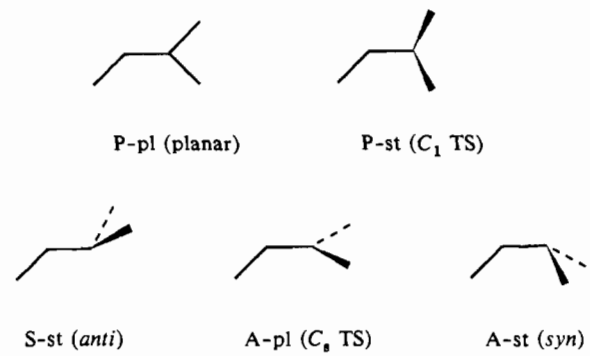

We found that the anomeric effect in the sulfenamides $XSNH_2$ involves unusually large energetic and geometric changes (see Table II and the discussion below). To facilitate further study of these species, we supply their remaining geometrical parameters in Table VII.

The stabilization energies of the most favorable A-st (syn) conformers of $FONH_2$ and $FSNH_2$ (16.8 and 18.7 kcal/mol) are large and are in the range of those for the C, N, and P compounds discussed above. The syn conformation of $FONH_2$ is 4.5 kcal/mol lower in energy than the anti (S-st) form, and there is a large internal rotation barrier to P-st (the C_1 transition structure, TS) of 12.1 kcal/mol with respect to *syn*-$FONH_2$. The inversion barrier at N is 9.0 kcal/mol to the C_s TS, A-pl. As seen in Table I, the N–O distance varies considerably, from 1.305 (C_s TS) to 1.342 (syn) to 1.360 (anti) to 1.416 Å (C_1 TS). By contrast, in hydroxylamine, anti is favored over syn by 5.6 kcal/mol, and the internal rotation and nitrogen inversion barriers are 8.7 and 14.1 kcal/mol, respectively. Thus, with respect to $HONH_2$, the inversion barrier in $FONH_2$ is smaller (even though the substituent electronegativity of –OF is *greater* than that of –OH), the rotation barrier larger, and the syn–anti preference reversed. Note that the inversion barrier of $HONH_2$ is greater than its rotation barrier, whereas the reverse is true for $FONH_2$. (In NMR spectroscopic investigations of hydroxylamines (and also other species), it is important to know the rough numerical relationship between barriers to rotation and inversion in order to interpret measured free energies of activation.[28b]) Though smaller than in $FONH_2$, the effects of hyperconjugation can nevertheless be seen in $HONH_2$: the N–O bond length shortens along the sequence S-st, A-st, and A-pl from 1.404 to 1.368 Å, with a corresponding lengthening of the O–H bond by 0.004 Å.

In the sulfur species in Table II,[32] the S–N single-bond lengths vary over the considerable range of 0.14 Å, from 1.755 Å in P-st $HSNH_2$ to 1.615 Å in A-pl $FSNH_2$. As in $HONH_2$, the anti conformer of $HSNH_2$ is favored over the syn, but in this case by only 0.53 kcal/mol. The syn conformer of $HSNH_2$ has a shorter S–N bond length (1.695 vs 1.710 Å) and wider NSH angle (102.6 vs 97.9°) than the anti conformer. From Tables III and IV, the inversion barrier of $HSNH_2$ is much smaller than that of $HONH_2$, both in the anti conformer and in the C_1 TS. This is mainly ascribable to the smaller electronegativity of SH (vs that of OH). In both $HONH_2$ and $HSNH_2$, the inversion barrier of the C_1 TS (i.e., energy difference between the A-st and fully planar A-pl stationary points) is considerably higher than that of the syn or

(36) (a) Holywell, G. C.; Rankin, D. W. H.; Beagley, B.; Freeman, J. M. *J. Chem. Soc. A* **1971**, 785–790. (b) "Typical" values of P–N double bonds in crystal structures are 1.54–1.55 Å; see: Pohl, S. *Chem. Ber.* **1979**, *112*, 3159–3165.
(37) Schomaker, V.; Stevenson, D. P. *J. Am. Chem. Soc.* **1941**, *63*, 37–40.
(38) Quantum Chemistry Archive, Friedrich-Alexander University, Erlangen-Nürnberg, FRG (unpublished).

Table VII. HF/6-31G* Optimized Structures of $XSNH_2$ Species[a]

	sym	conformn	$R(NH_a)$	$R(NH_b)$	$\theta(SNH_a)$	$\theta(SNH_b)$	$\theta(HNH)$	$\phi(FSNH_a)$
$HSNH_2$	C_s	P-pl	0.990	0.990	122.0	118.2	119.8	0.0
$HSNH_2$	C_1	P-st	1.002	1.003	109.0	106.4	105.7	23.8
$HSNH_2$	C_s	A-pl	0.992	0.992	120.6	120.6	118.8	
$HSNH_2$	C_s	A-st	0.998	0.998	113.7	113.7	111.3	
$HSNH_2$	C_s	S-st	0.999	0.999	111.2	111.2	110.0	
$FSNH_2$	C_s	P-pl	0.993	0.992	118.9	120.0	121.1	0.0
$FSNH_2$	C_s	A-pl[b]	0.994	0.994	120.4	120.4	119.2	90.0
$FSNH_2$	C_1	P-st	1.006	1.006	106.1	107.0	105.6	31.4
$FSNH_2$	C_s	A-pl[c]	0.995	0.995	121.2	121.2	117.5	90.0
$FSNH_2$	C_s	A-st	0.998	0.998	117.4	117.4	113.6	
$ClSNH_2$	C_s	P-pl	0.992	0.992	121.1	118.0	120.9	0.0
$ClSNH_2$	C_1	P-st	1.004	1.005	108.5	105.8	105.8	29.3
$ClSNH_2$	C_s	A-pl[c]	0.995	0.995	121.0	121.0	118.1	90.0
$ClSNH_2$	C_s	A-st	0.999	0.999	116.6	116.6	113.4	

[a] See Tables I and II for energies and remaining parameters. Bond lengths are in Å and angles in degrees. H_a is the H atom nearest to the F atom. [b] Geometry optimization carried out with respect to the *truncated* HF/6-31G* energy where the $n_N \rightarrow \sigma_{SF}^*$ interaction has been zeroed (see text). [c] Forced to be planar at N.

anti conformers (see Tables III, IV); this is due to the lack of $n_N \rightarrow \sigma_{AH}^*$ hyperconjugation at the transition structure for internal rotation.

The conformational properties of $FSNH_2$ are significantly different. In this case, the syn conformer is close enough to being planar at nitrogen that attempts to optimize a structure for the anti conformer led back to the syn conformer. Thus, there is no stationary point on the potential energy surface of $FSNH_2$ either for the anti conformer or for inversion at N, and the only minimum is the syn conformer. The internal rotation barrier (to the C_1 TS) was found to be 18.3 kcal/mol. Since hyperconjugation in $FSNH_2$ should be the strongest when the amino group is planar, we optimized an A-pl structure for $FSNH_2$ where the SNH_2 unit was held in a plane; we denote this as the *planar-SNH_2* structure. This is *not* a stationary point because there are nonzero forces on the hydrogen atoms. Surprisingly, the planar-SNH_2 structure is only 1.5 kcal/mol higher in energy than the syn structure. The inversion barrier for the C_1 TS of $FSNH_2$ (going to the fully planar structure) is 8.7 kcal/mol. Thus, the pyramidalization energy of the planar-SNH_2 structure is only a small fraction of that of the fully planar structure (1.5 vs 8.7 kcal/mol). Also, the degree of pyramidalization at N in the syn structure is much smaller than that in the C_1 TS (see Table II, 11.6 vs 41.3°). Large changes are seen also in the NSF angle, which increases from 95.1 to 103.9° on going from the fully planar to the syn structure. The variations in the S–N and S–F bond lengths are of prime interest, and they are in accord with strong $n_N \rightarrow \sigma_{SF}^*$ interaction. As one goes from the planar-SNH_2 to the C_1 TS structure of $FSNH_2$, the S–N bond distance increases by 0.118 Å and the S–F length decreases by 0.016 Å. These trends, which point to partial π_{SN} bond formation through strong negative hyperconjugation, were subjected to NBO analysis, as described in the next section.

It important to realize that the stabilization energy (eq 1) for $FSNH_2$ provides a measure of the *relative* strength of the anomeric effect in $FSNH_2$ in comparison to that in reference compound $HSNH_2$ (and also FSH). Twisting $HSNH_2$ to eliminate the nitrogen lone pair delocalization (this cannot be done in FSH, but delocalization of the $n_F \rightarrow \sigma_{SH}^*$ type is much weaker), we arrive at the following "corrected" estimate of the anomeric effect in $FSNH_2$:

$$FSNH_2 + SH_2 \rightarrow FSH + H_2NSH(C_1\ TS) \qquad \Delta E = 26.9\ \text{kcal/mol} \tag{2}$$

The data for the $ClSNH_2$ species in Tables II and IV show features analogous to those for $FSNH_2$. No anti conformer exists, the internal rotation barrier is very large (16 kcal/mol), and very similar variations in the S–N distance and XSN angle are seen. The only significant difference is that the sulfur–halogen bond length varies over a much greater range in $ClSNH_2$ than in $FSNH_2$: 0.054 vs 0.018 Å. This is due to the weakness of an S–Cl as compared to an S–F bond. NBO analysis shows that, due to the two opposing factors of energy and overlap, the $n_N \rightarrow \sigma_{SCl}^*$ interaction in $ClSNH_2$ is of roughly the same energy as the $n_N \rightarrow \sigma_{SF}^*$ interaction in $FSNH_2$: Though the σ_{SCl}^* orbital is much lower in energy than σ_{SF}^* (a consequence of the reduced bond energy), the polarization of σ_{SCl}^* toward S is much smaller than that of σ_{SF}^*, and thus n_N–σ_{SCl}^* overlap is poorer than n_N–σ_{SF}^* overlap. (The numerical values are presented in the next section.)

G. NBO Analysis of $FSNH_2$. 1. Perturbative Analysis of $n_N \rightarrow \sigma_{SF}^*$ Interaction. NBO analysis of $FSNH_2$ wave functions strongly supports the postulated negative hyperconjugation origin of the large internal rotation barrier. The predominance of $n_N \rightarrow \sigma_{SF}^*$ delocalization stands out in the NBO analysis. The n_N and σ_{SF}^* NBO occupancies in the planar-SNH_2 structure are 1.890e and 0.094e, respectively. These are the orbitals in the NBO analysis whose occupancies deviate by far the most from the ideal Lewis values of 2.0 for bonds and lone pairs and 0.0 for antibonds and "Rydberg" orbitals. In fully planar $FSNH_2$, these occupancies are much closer to the ideal localized values, taking values of 1.991 (n_N) and 0.012 (σ_{SF}^*). The strength of the interaction between the n_N and σ_{SF}^* NBOs in the planar-SNH_2 structure of $FSNH_2$ is shown by the large magnitude of the Fock matrix element connecting these two orbitals (0.144 au). The n_N–σ_{SF}^* orbital energy difference, 0.73 au, leads to an estimate of −35 kcal/mol by second-order perturbation theory[13d] for this interaction. This value is comparable to the energy difference of 27 kcal/mol between the planar-SNH_2 and fully planar structures. (For the $n_N \rightarrow \sigma_{SCl}^*$ interaction in the planar-SNH_2 structure of $ClSNH_2$, the corresponding values are as follows: NBO Fock matrix element, 0.128 au; orbital energy difference, 0.60 au; perturbative energy estimate, −34 kcal/mol. Refer to the discussion of $ClSNH_2$ in the previous section.) However, the magnitude of this interaction is so large that it is overestimated significantly by second-order perturbation theory. A more realistic estimate of the $n_N \rightarrow \sigma_{SF}^*$ interaction energy may be obtained through the NBO Fock matrix deletion procedure, as described below.

2. Fock Matrix Deletion Analysis. By zeroing the n_N–σ_{SF}^* NBO Fock matrix element and carrying out the deletion procedure (see section II), we find that the total energy of the planar-SNH_2 structure of $FSNH_2$ increases by 24 kcal/mol. As a result of the deletion of the $n_N \rightarrow \sigma_{SF}^*$ interaction in the planar-SNH_2 structure of $FSNH_2$, the occupancy of the n_N NBO increases by 0.096 to 1.986 and that of σ_{SF}^* decreases by 0.088 to 0.006; these occupancies are similar to those listed above for the fully planar structure where the interaction is absent. (Application of the deletion procedure to the fully planar structure leads to no change in the occupancies or energy.) The only other significant occupancy change during this deletion is that of the most highly occupied sulfur Rydberg NBO (denoted as r_S), which decreases by 0.009. Before the deletion, r_S has an occupancy of 0.021, has 80% d character, and interacts with the nitrogen lone pair in what can be regarded as p→d π_{NS} bonding (the $n_N \rightarrow r_S$ second-order energy is −8.6 kcal/mol). The existence of a small coupling

between the $n_N \rightarrow \sigma_{SF}^*$ and $n_N \rightarrow r_S$ interactions is reasonable since both of these interactions are sizable and involve donation from the nitrogen lone pair into orbitals on sulfur. Coupling with other delocalization interactions is insignificant, and therefore, the $n_N \rightarrow \sigma_{SF}^*$ deletion energy of 24 kcal/mol can be regarded as providing a trustworthy estimate of the strength of this interaction.

3. Localized Molecular Orbital Analysis. A direct description of the π_{SN} partial bond formation in $FSNH_2$ is provided by the delocalization tail[13c] of the localized molecular orbital (LMO) corresponding to the nitrogen lone pair. As described in section II, the LMO method directly connected with NBO analysis is called "natural LMOs" (NLMOs).[13c] Through this analysis, the nature of the delocalization of the nitrogen lone pair can be examined more explicitly. The NLMO corresponding to the n_N NBO in the planar-SNH_2 structure of $FSNH_2$ is composed 94.5% from a hybrid on nitrogen of 99.9% p character and has a delocalization tail of 5.5% onto the other atoms: 4.5% onto a hybrid on sulfur and 1.0% onto a hybrid on fluorine of opposite phase (i.e., the delocalization tail involves N–S bonding and S–F antibonding character). By this analysis, 4.5% × 2 = 9.0% of a covalent π_{SN} bond is formed in the NSF plane. Due to the aforementioned $n_N \rightarrow r_S$ interaction, the amount of d character in the *sulfur* hybrid of the n_N NLMO (11%) is much greater than the amount of d character in the *sulfur* hybrid of the σ_{SF}^* NBO into which the n_N NBO delocalizes (2%), and the ratio of sulfur to fluorine contributions to the n_N NLMO (4.5) is somewhat greater than in the σ_{SF}^* NBO (3.7). By contrast, the corresponding *fluorine* hybrids in the σ_{SF}^* NLMO and in the n_N NBO are quite similar. Interestingly, the amount of s character in the sulfur hybrid of the n_N NLMO (5%) is only one-third of that in the sulfur hybrid of the σ_{SF}^* NBO, and this lost s character is replaced by d character (from r_S) of π-symmetry with respect to the S–N bond. The nitrogen lone pair thus prefers to delocalize into a hybrid on sulfur of somewhat greater π-character with respect to the S–N bond than that offered to it by the σ_{SF}^* orbital and delocalizes to some extent in the sulfur d orbital (r_S). In contrast to the $n_N \rightarrow \sigma_{SF}^*$ interaction, the $n_N \rightarrow r_S$ interaction can have only a very weak dependence on rotation about the S–N bond. Hence, in studying the factors affecting the stability of the various molecular conformations of $FSNH_2$, one can ignore the r_S contribution to the nitrogen lone pair delocalization.

4. Reoptimization of Geometry with Hyperconjugation Eliminated. In order to ascertain the full extent of the influence of nitrogen lone pair hyperconjugation on the molecular geometry, we reoptimized the geometry of the planar-SNH_2 (A-pl) structure with this interaction eliminated. Specifically, the geometry was varied in order to minimize the energy obtained from the deletion procedure after zeroing the $n_N \rightarrow \sigma_{SF}^*$ Fock matrix element. The results are given in Tables II and VII (see the footnoted entries for A-pl $FSNH_2$ in these tables): The optimized deletion energy is still 4.8 kcal/mol *below* the total energy of the fully planar structure of $FSNH_2$. The reoptimization of the geometry of the planar-SNH_2 structure of $FSNH_2$ resulted in a lengthening of the S–N bond by 0.077 Å, yielding a value (1.692 Å) that is still 0.006 Å *less* than that in the fully planar structure. Additionally, the S–F bond is contracted by 0.028 Å, the HNH angle increased by 1.7°, and the NSF angle decreased by 3.0°. Indeed, as a result of the reoptimization, all geometrical parameters have stepped significantly toward the values that they assume in the fully planar structure.

5. Interplay of Hyperconjugation with Pyramidalization at N. In the syn structure, the $n_N \rightarrow \sigma_{SF}^*$ interaction is somewhat weaker, and these orbitals have occupancies of 1.904 (n_N) and 0.085 (σ_{SF}^*). This is due to the pyramidalization at N, which results in the mixing of 9% s character into the n_N NBO, in the decrease of the off-diagonal Fock matrix element for this interaction to 0.134 au, and in the increase of the orbital energy difference to 0.77 au. Therefore, somewhat smaller perturbative (−29 kcal/mol) and Fock matrix element deletion (−21 kcal/mol) energies are found than in the case of the planar-SNH_2 structure. In order to examine the interplay of hyperconjugation and pyramidalization in more detail, we reoptimized the angles at N with respect to the deletion energy obtained after zeroing the $n_N \rightarrow \sigma_{SF}^*$ element, starting with the fully optimized syn structure. As a result of this partial reoptimization, the SNX angle (the NX vector being the bisector of the HNH angle) was reduced from 147.1 to 131.5° and the HNH angle from 113.6 to 108.6° ($\Delta\theta$(N) thus was increased from 12 to 26°), and the deletion energy was lowered by 1.3 kcal/mol. This illustrates the competition between n_N hyperconjugation and pyramidalization in $FSNH_2$: $n_N \rightarrow \sigma_{SF}^*$ interaction forces greater planarity at N. From the NLMO analysis, the nitrogen lone pair is 4.8% delocalized and the π_{SN} covalent bond order is 0.079 in the syn structure. This compares with a π_{SN} covalent bond order of 0.090 in the planar-SNH_2 structure (cf. the value of 9.0% in section III-G3 above).

6. Orbital Overlap and NSF Angle. It is informative to examine the value of the $n_N \rightarrow \sigma_{SF}^*$ orbital overlap directly, for Fock matrix elements are often roughly proportional to orbital overlap.[2c] Since the NBOs are orthogonal, the overlap must be examined in the basis of the preorthogonal NBOs (pre-NBOs), as discussed in our previous work.[2c] As expected, the n_N–σ_{SF}^* pre-NBO overlap is greater in the planar-SNH_2 than in the syn structure (0.181 vs 0.174). Though the difference between these two values is small, the squares of these overlaps (which enter the second-order energy formula[2c]) differ by nearly 10%, and this leads to a difference of hyperconjugative energies of around 2–3 kcal/mol. It is important to mention that the 0.174 value of n_N–σ_{SF}^* overlap in *syn*-$FSNH_2$ is the *difference* between the overlap of n_N with the sulfur and with the fluorine hybrid components of σ_{SF}^*, these overlap components being +0.196 and −0.022. When the NSF angle is decreased, the magnitude of the negative fluorine hybrid component of the overlap increases somewhat faster than does that of the positive sulfur component. (Note that when the acceptor antibond is less polarized toward the central atom, as, for instance, is the case for $n_F \rightarrow \sigma_{CH}^*$ interactions in CH_3F, the $n \rightarrow \sigma^*$ overlap cancellation upon angle decrease is much stronger.[2c]) When the NSF angle is changed to the value that it assumes in the fully planar structure (95.1°), the n_N–σ_{SF}^* pre-NBO overlap decreases to 0.168 = 0.198 − 0.030. The second-order and Fock matrix deletion energies for this delocalization decrease in magnitude by 3.6 and 3.1 kcal/mol, respectively. The effect is not very large because the σ_{SF}^* orbital has only a small (21%) component on fluorine, but it is responsible for the 3.0° decrease in the NSF angle in the planar-SNH_2 structure (A-pl) upon deleting the $n_N \rightarrow \sigma_{SF}^*$ interaction (Table II). The NSF angle could also be widened by n_N–σ_{SF} repulsive interaction, and we find the n_N–σ_{SF} pre-NBO overlap in *syn*-$FSNH_2$ to increase from 0.144 to 0.160 upon changing the NSF angle from its optimum value (103.9°) to 95.1°. Indeed, from the above data, it is found that the ratio of the square of n_N–σ_{SF}^* pre-NBO overlap to the square of n_N–σ_{SF} pre-NBO overlap decreases sharply from 1.46 to 1.10 upon reducing the NSF angle from 103.9 to 95.1°.

Since there is some coupling between the $n_N \rightarrow \sigma_{SF}^*$ and $n_N \rightarrow r_S$ interactions (where r_S is a π-type "Rydberg" orbital on sulfur of primarily 3d character), we reoptimized the NSF angle in the planar-SNH_2 structure with respect to the deletion of the NBO Fock matrix elements for both of these interactions, leaving all other geometrical parameters at their optimum HF/6-31G* values. The NSF angle was found to decrease to 99.1°, which is approximately halfway between the values in planar-SNH_2 (103.8°) and in fully planar $FSNH_2$ (95.1°). We therefore ascribe roughly half of the NSF angle increase to the influence of negative hyperconjugation and the other half to other factors, which could include n_N–σ_{SF} repulsion.

7. Quantitative Description of Rotation Barrier. We turn now to the quantitative description of the internal rotation barrier in $FSNH_2$, considering the role of all possible delocalization interactions. For this purpose, it is most convenient to compare the planar-SNH_2 and the fully planar structures, thereby avoiding the complications that arise in the syn and C_1 TS structures due to the pyramidalization at nitrogen. The additional problems associated with the large bond length and bond angle changes that occur during internal rotation are avoided by examining the rigid rotation of the planar-SNH_2 structure to an unrelaxed, fully planar

Table VIII. Rigid Rotation of planar-SNH_2 Structure of $FSNH_2$ to a Planarized Structure (pl-pl-SNH_2): NBO Energetic Analysis[a]

energy quantity	pl-SNH_2	pl-pl-SNH_2	Δ
E(rel)	0.0	+31.1	+31.1
E_L(rel)[b]	0.0	−2.2	−2.2
E_D[c]	−89.2	−56.0	+33.2
$E(\sigma_{SF}\rightarrow 2\sigma_{NH}^*)$[d]	−0.2	−1.5	−1.3
$E(2\sigma_{NH}\rightarrow\sigma_{SF}^*)$[d]	−0.0	−5.0	−5.0
$E(\sigma_S\rightarrow 2\sigma_{NH}^*)$[d]	−7.8	−7.9	−0.1
$E(\pi_S\rightarrow 2\sigma_{NH}^*)$[d]	−15.1	−0.0	+15.1
$E(n_N\rightarrow\sigma_{SF}^*)$[d]	−23.9	−0.0	+23.9
$E(\pi_F\rightarrow\sigma_{SN}^*)$[d]	−7.4	−6.6	+0.8
$E(\pi_F\rightarrow 2\sigma_{NH}^*)$[d]	−0.0	−0.5	−0.5
$E(n,\sigma\rightarrow\sigma^*)$[e]	−54.4	−21.5	+32.9
$E(n_N\rightarrow\sigma_{SF}^*,r_S)$[d]	−34.5	−8.3	+26.2

[a] See text for details; energies are in kcal/mol. [b] Energy of localized NBO Lewis structure. [c] Energy of delocalization from NBO Lewis structure. [d] Delocalization energy for specific interactions estimated by zeroing the corresponding Fock matrix elements. [e] Total of energies for the major individual lone pair or bond to antibond delocalizations (all lines with footnote *d* except the last line of the table are summed).

structure, which we shall denote as the planarized-planar-SNH_2 (pl-pl-SNH_2) form. The pl-pl-SNH_2 structure was found to be 31 kcal/mol higher in energy than planar-SNH_2; this value corresponds to the barrier for a rigid internal rotation process with no relaxation of bond lengths and angles.

The rigid rotation barrier ΔE was decomposed by NBO Fock matrix deletion analysis, and the results are summarized in Table VIII. First, all antibond and Rydberg orbitals were deleted from the NBO Fock matrix for both structures. This forces the electrons to fully occupy the Lewis structure (consisting of core, lone pair, and bond NBOs) and gives the localized energy E_L. The total energetic contribution E_D from delocalization into antibond and Rydberg orbitals is given by the difference between the total energy E and the localized energy E_L. The contributions of E_L and E_D to the rigid internal rotation barrier of the planar-SNH_2 structure are $\Delta E_L = -2$ and $\Delta E_D = +33$ kcal/mol. Thus, ΔE_L is negligible and ΔE is accounted for nearly quantitatively by the delocalization energy component ΔE_D.

We decomposed the delocalization energy contribution E_D to the rigid rotation barrier ΔE by deleting individual Fock matrix elements (or pairs of them if the N–H bonds or antibonds were involved). As seen in Table VIII, the $n_N\rightarrow\sigma_{SF}^*$ interaction provides the largest contribution (24 kcal/mol) to ΔE_D; the 15 kcal/mol contribution from the $\pi_S\rightarrow 2\sigma_{NH}^*$ interaction is also quite significant. That the sum of these two contributions (39 kcal/mol) exceeds ΔE_D by 6 kcal/mol is due to the presence of stronger $\sigma_{SF}\rightarrow 2\sigma_{NH}^*$ and $2\sigma_{NH}\rightarrow\sigma_{SF}^*$ delocalization in the pl-pl-SNH_2 structure (Table VIII). Thus, we have a satisfactory quantitative description of the internal rotation barrier of $FSNH_2$ in terms of the contributions from various delocalization interactions. Note finally from Table VIII that deletion of the $n_N\rightarrow\sigma_{SF}^*$ and $n_N\rightarrow r_S$ interaction elements simultaneously yields a slightly greater contribution to ΔE_D than deletion of $n_N\rightarrow\sigma_{SF}^*$ alone (26 vs 24 kcal/mol, respectively).

The secondary hyperconjugative interaction $\pi_S\rightarrow 2\sigma_{NH}^*$ contributes surprisingly strongly to the rotation barrier and warrants further comment. The NLMO for the π_S lone pair is 0.5% delocalized onto N and 0.6% delocalized onto each of the hydrogens. This corresponds to the formation of 1.0% of a covalent π_{SN} bond, or a bond order of 0.01, compared to the π_{SN} bond order of 0.09 arising from the $n_N\rightarrow\sigma_{SF}^*$ interaction. Although the sulfur lone pair hyperconjugation is of some energetic importance, nitrogen lone pair hyperconjugation provides the dominant contribution to the S–N bond order increase and bond length contraction. Note that $\pi_S\rightarrow\sigma_{NH}^*$ interaction will occur also in $HSNH_2$. Thus, when $FSNH_2$ and $HSNH_2$ are compared, this interaction does not need to be considered.

8. Relationship between Bond Length and Bond Order. Interestingly, the contraction of the S–N bond by 0.083 Å as one goes from the fully planar (P-pl) to the planar-SNH_2 (A-pl) structure of $FSNH_2$ is associated with a total increase of only 0.10 in the S–N π-bond order. The HF/6-31G* S–N bond lengths in doubly bonded SNH and in triply bonded SN^+ are 1.539 and 1.397 Å,[38] respectively. If the S–N bond length of 1.710 Å in *anti*-$HSNH_2$ is taken as the "ideal" S–N single-bond length, the S–N bond length in the planar-SNH_2 structure of $FSNH_2$ (1.615 Å) is roughly halfway between the single- and double-bond values, implying a *geometric* bond order of around 1.50 (this case is similar to F_2PNH_2; see section III-E). Thus, bond lengths are clearly not proportional to bond orders when strong hyperconjugation is present. In accordance with our companion study on F_nAH_m molecules,[2c] an electrostatic (charge withdrawal) effect can be seen on the S–N bond length due to fluorine having much greater electronegativity than hydrogen: The S–N bond lengths in the fully planar and C_1 TS structures of $FSNH_2$ are contracted by 0.015 and 0.022 Å, respectively, in comparison with the analogous structures of $HSNH_2$ (see Table II).

H. Effect of Electron Correlation. The influence of correlation on the relative energies of the $FSNH_2$ and $ClSNH_2$ structures was investigated at the MP2/6-31G* (frozen core) level, at the HF/6-31G* geometries. For $FSNH_2$, the planarization energy at N (i.e., the relative energy of A-pl) decreases from 1.5 to 1.2 kcal/mol, the internal rotation barrier (relative energy of P-st) increases from 18.3 to 20.2 kcal/mol, and the planarization energy (relative energy of P-pl) increases from 27.0 to 30.2 kcal/mol (thus, the inversion barrier of the C_1 TS increases from 8.7 to 10.0 kcal/mol). The influence of correlation in the case of $ClSNH_2$ is very similar: the planarization energy at N decreases from 1.8 to 1.5 kcal/mol, the rotation barrier increases from 15.9 to 17.6 kcal/mol, the planarization energy increases from 24.3 to 27.2 kcal/mol, and the inversion barrier of the C_1 TS increases from 8.4 to 9.6 kcal/mol. The inclusion of electron correlation thus has little qualitative influence, leading to roughly 10% increases in the rotation barriers.

We further investigated the effect of electron correlation on the geometries of FCH_2NH_2, $HSNH_2$, and $FSNH_2$, as summarized in Table IX, where the HF/6-31G* results are also listed for ease of comparison (full details are given in the supplementary material). As seen from Table IX, the relative energy of the conformers changes little on going from HF/6-31G*//HF/6-31G* to MP4SDTQ/6-31+G*//MP2FU/6-31G*, and the rotation barriers increase slightly. MP2FU/6-31G* geometry optimization has practically no effect on the internal rotation barrier of $FSNH_2$, which changes from 20.21 to 20.44 kcal/mol on going from MP2FC/6-31G*//HF/6-31G* to MP2FU/6-31G*//MP2FU/6-31G* (Table IX). The major geometrical change at MP2FU/6-31G* is the lengthening of the A–F bonds, which is in line with the general experience that bond lengths between nonelectropositive elements and fluorine are much too short at the SCF level.[30c] The relative values of R(AF) and the other geometric parameters among different conformers of the same species are qualitatively unchanged, however. Indeed, examination of Table IX reveals that the energetic and geometric effects ascribed to negative hyperconjugation are mildly *increased* in magnitude at the correlated level. For $FSNH_2$, for instance, the HF [MP2FU] values for the change as one goes from the A-st (syn) to the P-st (C_1 TS) structure are +18.3 kcal/mol [+20.4 kcal/mol] for ΔE, +0.102 Å [+0.123 Å] for ΔR(AN), −0.017 Å [−0.028 Å] for ΔR(AF), +29.8° [+37.1°] for $\Delta\Delta\theta$(N), and −7.7° [−9.8°] for $\Delta\theta$(FAN).

I. Comparison with MNDO and AM1 Methods. FCH_2NH_2 and $FSNH_2$ were optimized with MNDO[31a-c] and AM1[31d,e] in order to judge the performance of these semiempirical methods (see Table IX). In all cases, the potential energy surface with respect to internal rotation was qualitatively incorrect. For $FSNH_2$, a minimum structure was found by MNDO (i.e., the anti conformer) that does not exist at the ab initio level, and the rotation barrier was found to be only 5.7 kcal/mol. In discussing the results for FCH_2NH_2, we denote the conformation by the n_N–CF dihedral angle, ϕ, and give the relative energies of the structures in parentheses. As a function of ϕ, the ab initio surface has the global minimum at 180° (A-st), a transition structure (TS) at 90° (8–9 kcal/mol; P-st), and a second, shallow minimum at 0° (5 kcal/mol;

Table IX. Summary of Geometries and Energies for Selected $F_nAH_mNH_2$ Species at Other Levels of Theory, Compared with the HF/6-31G* Level[a]

	sym	conformn	level	E	E_{rel}	R(AN)	R(AF)[b]	$\Delta\theta$(N)	θ(FAN)[b]
FCH_2NH_2	C_1	P-st	HF/6-31G*	−194.060 49	7.77	1.441	1.364	31.9	108.4
			MP2FU/6-31G*	−194.532 59	8.85	1.453	1.390	36.0	108.2
			MP4SDTQ/6-31+G*[c]	−194.582 14	8.88				
			MNDO	−55.95[d]	2.52[e]	1.475	1.350	31.8	110.3
			AM1	(−54.63)[d,f]	(3.91)[f]	no stationary point			
FCH_2NH_2	C_s	A-pl	HF/6-31G*	−194.063 94	5.61	1.397	1.378	3.4	112.6
			MP2FU/6-31G*	−194.537 38	5.84	1.401	1.410	5.6	112.6
			MP4SDTQ/6-31+G*[c]	−194.588 42	4.94				
			MNDO	−51.40[d]	7.07	1.437	1.356	0.6	109.7
			AM1	−52.57[d]	5.96	1.425	1.393	5.9	112.2
FCH_2NH_2	C_s	A-st	HF/6-31G*	−194.072 88	0.00	1.412	1.379	28.4	113.1
			MP2FU/6-31G*	−194.546 69	0.00	1.417	1.411	32.8	113.6
			MP4SDTQ/6-31+G*[c]	−194.596 29	0.00				
			MNDO	−58.47[d]	0.00	1.467	1.357	30.4	112.1
			AM1	−58.54[d]	0.00	1.443	1.395	17.9	115.0
$HSNH_2$	C_1	P-st	HF/6-31G*	−453.660 72	8.23	1.755	1.325	38.9	97.4
			MP2FU/6-31G*	−453.959 95	8.78	1.780	1.340	43.3	96.7
$HSNH_2$	C_s	A-st	HF/6-31G*	−453.673 84	0.53	1.695	1.334	21.5	102.6
			MP2FU/6-31G*	−453.972 37	0.99	1.710	1.353	23.8	103.0
$HSNH_2$	C_s	S-st	HF/6-31G*	−453.674 69	0.00	1.710	1.326	27.7	97.9
			MP2FU/6-31G*	−453.973 94	0.00	1.731	1.341	32.2	97.0
$FSNH_2$	C_1	P-st	HF/6-31G*	−552.486 50	18.27	1.733	1.609	41.3	96.2
			MP2FC/6-31G*	−552.943 62	20.21				
			MP2FU/6-31G*	−552.962 20	20.44	1.756	1.642	46.4	95.8
			MP4SDTQ/6-31+G*[c]	−553.008 59	19.51				
			MNDO	−19.34[d]	5.70	1.671	1.573	13.0	103.3
$FSNH_2$	C_s	S-st	HF/6-31G*			no stationary point			
			MNDO	−23.97[d]	1.07	1.641	1.577	27.2	100.8
$FSNH_2$	C_s	A-st	HF/6-31G*	−552.515 61	0.00	1.631	1.626	11.6	103.9
			MP2FC/6-31G*	−552.975 82	0.00				
			MP2FU/6-31G*	−552.994 78	0.00	1.633	1.670	9.3	105.6
			MP4SDTQ/6-31+G*[c]	−553.039 68	0.00				
			MNDO	−25.04[d]	0.00	1.630	1.584	21.0	104.8

[a] Notation and units same as in Tables I and II. [b] The A–H bond lengths and θ(HAN) angles are given for nonfluorinated species. [c] At MP2FU/6-31G* geometry. [d] Heat of formation in kcal/mol. [e] The eclipsed conformer (S-ec) is *higher* in energy, at 3.19 kcal/mol (both are transition states); see text. [f] Optimized energy with one FCNH angle fixed at the MNDO value. The transition state for internal rotation is the eclipsed conformer (S-ec), at 5.83 kcal/mol; see text.

S-ec). The MNDO surface has indeed its global minimum at 180° and a TS at 90° (+2.52 kcal/mol), but it has a shallow minimum at 60° (+2.23 kcal/mol) and a *second*, higher TS at 0° (3.19 kcal/mol). With AM1, the TS at 90° fully disappears (optimization with ϕ fixed at about 90° yields a relative energy of +3.91 kcal/mol), and the "TS" at 0° rises to +5.83 kcal/mol. The poor performance of MNDO and AM1 for the anomeric effect is not surprising when the inaccuracy of these methods for the rotation barriers of ethane and formamide is considered.[31a,d] Baird[31f] previously noted the bad performance of MNDO for the fluoromethane series.

IV. Discussion of Related Systems Studied Experimentally

A. General Remarks. Not every species that is strongly stabilized by negative hyperconjugation will be chemically stable, and all possibilities on the global free energy surface must be considered, including decomposition reactions with mono- and bimolecular mechanisms. Indeed, very few of the fluoroamine compounds discussed here are known, and even those that have been synthesized undergo decomposition: F_2BNH_2,[19d] F_3CNH_2,[23] and F_2PNH_2.[20] F_3CNH_2, for example, readily loses two molecules of HF[23] (as discussed in section III). Of the fluorinated molecules considered in this work, it is found from the HF/6-31G*//HF/6-31G* energies in Tables I and II and ref 32 and 38 that three have *exothermic* decomposition energies ΔE with respect to loss of one (in the case of monofluoro species) or two (in the case of di- and trifluoro species) molecules of HF (ΔE values in kcal/mol): $FNHNH_2$ (−20), F_2NNH_2 (−122), and $FONH_2$ (−46). These ΔE values reflect the weakness of N—F and O—F bonds in comparison to H—F, N=N, N≡N, and N=O bonds. For many of the other species, the decomposition energy values ΔE are found at HF/6-31G*//HF/6-31G* to be *less* endothermic than for F_3CNH_2 (+70 kcal/mol): $FSNH_2$ (+34), FCH_2NH_2 (+26), F_2CHNH_2 (+37), $FPHNH_2$ (+59), and F_2BNH_2 (+66, to BN singlet). (These values could change significantly with inclusion of correlation.) Though energy barriers for HF loss may be large, such energetic relationships should be kept in mind if syntheses are attempted. It is only in the cases of the fluoroamines of Al and Si that the ΔE values for HF loss are more endothermic than 100 kcal/mol.

The experimental results for F_2BNH_2, F_3CNH_2, and F_2PNH_2 have been discussed already in section III. We extend our discussion in this section to various other experimentally known systems in which hyperconjugative effects occur that are analogous to those in the $F_nAH_mNH_2$ species studied in this work. This constitutes a brief survey of negative hyperconjugation at B, C, N, O, Al, Si, P, and S centers.

B. B and Al Centers. Though negative hyperconjugation is weak at B and Al centers, there are experimentally observable consequences. A boron-centered anomeric effect has recently been observed for the first time, involving oxygen lone pair to B–Cl antibond interaction.[39] In addition, a hyperconjugative $n_N \rightarrow \sigma_{AlH}^*$ model has been employed to relate aluminum hydride ESR coupling constants with the coordination geometry of radical complexes formed from reaction of AlH_3 with N-heterocycles.[40] Another system which may involve hyperconjugation at aluminum is that of the salt $K^+Et_3AlFAlEt_3^-$, for which an X-ray analysis yields a linear Al–F–Al unit with symmetrical Al–F bonds of 1.80

(39) Shiner, C. S.; Gardner, C. N.; Haltiwanger, R. C. *J. Am. Chem. Soc.* **1985**, *107*, 7167–7172; **1987**, *109*, 4129.
(40) Kaim, W. *J. Am. Chem. Soc.* **1984**, *106*, 1712–1716.

± 0.06 Å.[41a] To account for the unexpectedly short Al–F distances to the bridging fluoride ion, Natta et al.[41a] proposed a bonding model where the fluorine lone pairs donate into aluminum 3d orbitals. A model involving $\pi_F \rightarrow \sigma_{AlC}^*$ interaction, in addition to strongly ionic Al–F σ bonding, would be more appropriate. An analogous system involving a linear Al–O–Al unit with symmetrical and short (1.68 Å) Al–O bonds is $[(C_{10}H_8NO)_2Al]_2O$, where each aluminum is pentacoordinate and forms bonds to the N and O atoms of two 2-methyl-8-quinolinolato ligands.[41b] The 3d orbitals of aluminum were again thought to be of great importance,[41b] but it would be better to postulate significant $\pi_O \rightarrow \sigma_{AlX}^*$ (X = N, O) interaction instead.

Although aminoboranes X_2BNR_2 tend to form dimers and trimers, they can be observed as monomers, and the unsubstituted species X_2BNH_2 exist as transient intermediates.[19d] Aminoalane species X_2AlNR_2 have a yet greater drive toward oligomerization, due to the greater electropositivity of Al, and monomers are not observed.[42] Various alkyl-substituted species Cl_2AlNR_2 have been found as dimers.[42b-d] However, the triamino-substituted alane $[((H_3C)_3Si)_2N]_3Al$ was isolated as a monomer.[42e] Due to the steric bulk of the substituents, the NSi_2 planes are skewed by 50° with respect to the N_3Al plane; hence, both direct π(N–Al) and hyperconjugative $n_N \rightarrow \sigma^*$(Al–N) bonding can occur. The Al–N bond lengths were found to be 1.78 Å, which is in the range of the Al–N bond lengths given in Table II.

C. C and Si Centers. Anomeric effects in organic amines are well-established.[1,2a,b] As already discussed, primary α-fluoroamines readily eliminate HF and are unstable.[23] Tertiary α-fluoroamines are known, and the structure of the simplest of these species, $(F_3C)_3N$, has been roughly determined by electron diffraction, with CNC angles of 114 ± 3°.[43a] Reinvestigation of this species would be desirable, particularly with regard to the degree of planarity at nitrogen. After this work had been submitted, an experimental NMR study appeared in which the rotation–inversion activation barriers ($\Delta G^{\ddagger}$) of two *N*-alkyl-substituted fluoroamines, FCH_2NRCH_3, were determined to be 10.1 kcal/mol.[29] This value is somewhat higher than our value ΔE = 8.9 kcal/mol for the rotation barrier of FCH_2NH_2 at the MP4SDTQ/6-31+G*//MP2FU/6-31G* level (note from Table IX that this value is raised by about 1 kcal/mol by electron correlation). Direct comparison of this value with experiment would require the consideration of solvation and entropy effects and an estimation of the magnitude of barrier increase to be expected due to *N*-alkyl substitution. Due to steric effects, the inversion barrier of FCH_2NRCH_3 (R = Et, CH_2Ph) will be significantly greater than that of FCH_2NH_2 (which from Table IX is 4.9 kcal/mol) and should be roughly similar to the inversion barrier $\Delta G^{\ddagger}$ of $F_3CCH_2NRCH_3$ (R = CH_2Ph) of 7.9 kcal/mol[29] determined from NMR measurements. Simple α-fluoroamines are highly reactive, and due presumably to the weakening of the C–F bond and the strengthening of the C–N bond through negative hyperconjugation, they undergo rapid fluoride exchange at room temperature even in nonpolar solvents, as seen by the absence of geminal F–H coupling in NMR spectra.[29,43b]

Much different behavior is exhibited by α-chloro and α-bromo amines, which exist in solution as imonium salts.[1,43c] Here, the influence of the solution facilitates the complete nucleophilic displacement of halide ion from the carbon center by the nitrogen lone pair with formation of a C=N bond. Covalent α-halo amines are only found when the nitrogen lone pair is constrained from assuming an anti conformation with respect to the C–X bond in a polycyclic ring system.[43c] From our comparison of $FSNH_2$ and $ClSNH_2$, $n_N \rightarrow \sigma_{CCl}^*$ interaction can be expected to have an energy roughly similar to that of $n_N \rightarrow \sigma_{CF}^*$, but with correspondingly greater weakening and stretching of the carbon–halogen bond. A still better electron acceptor than σ_{CX}^* (X = halogen) is π_{CO}^*, as it is quite polar and also has lower energy. The prime example of $n_N \rightarrow \pi_{CO}^*$ interaction is that of formamide, H_2NCHO, which by experiment and theory is nearly planar.[22,44] Here, negative hyperconjugation becomes undistinguishable from traditional models of π-resonance. (It should be pointed out that hyperconjugation of $n_N \rightarrow \sigma_{CO}^*$ type will occur in the transition state for internal rotation of formamide, reducing the barrier. The energetic contribution of π-resonance to planar formamide is therefore underestimated by the rotation barrier.) One can also consider changing the donor orbital in $n_N \rightarrow \sigma_{CF}^*$ from n_N to π_{NN}, for instance, which should be a more powerful donor. Such $\pi_{NN} \rightarrow \sigma_{CF}^*$ interactions are important in perfluorodiazirene, F_2CN_2, where the π_{NN} orbital in the three-membered CN_2 ring can strongly interact with the antisymmetric combination of the two σ_{CF}^* orbitals. The strong hyperconjugation interaction is reflected in the experimental geometry of this molecule,[45] where, in comparison with the corresponding nonfluorinated compound H_2CN_2, the N=N bond is lengthened by 0.06 Å and the two C—N bonds are shortened by 0.06 Å. We have confirmed this interpretation by NBO analysis at the HF/3-21G level and find a loss of around 0.12e from π_{NN} into the C–F antibonds. A carbanionic lone pair π_C is also a better donor than n_N, and strong geometric effects due to $\pi_C \rightarrow \sigma_{CF}^*$ interaction are apparent in the first experimentally determined structure of a polyfluoro carbanion:[7c] the carbanion center C_α is planar, with C_α–C "single" bond lengths of 1.43–1.44 Å and C_αCF angles of 120°. These geometric features were also well-reproduced by ab initio calculations.[7c]

Many (fluorosilyl)amine compounds of type $F_nSiH_m(NR_2)_p$ (n = 1–3; p = 1–3) have been synthesized,[46] including the rather stable polymer $(-F_2Si-NH-)_n$,[46e] and some of these have proven synthetically useful.[46] Grosse-Ruyken and Kleesaat[46a] prepared the first species of this class, $F_3SiN(CH_3)_2$, which decomposes slowly to give SiF_4. The structure of $F_3SiN(CH_3)_2$, as also that of $Cl_3SiN(CH_3)_2$, was determined by Airey et al.[46g] to be planar at nitrogen. It was noted by Grosse-Ruyken and Kleesaat[46a] that this molecule is a significantly weaker Lewis acid than SiF_4: $F_3SiN(CH_3)_2$ forms 1:1 gas-phase complexes with amines whereas SiF_4 forms 1:2 complexes. Additionally, Wannagat et al.[46b] found that the *N*-silyl-disubstituted species $(Me_3Si)_2N-SiF_3$ did not form adducts with amines, in contrast with the behavior of other F_3Si– derivatives. These workers concluded from the IR and NMR spectra of $(Me_3Si)_2N—SiX_3$ compounds that the N=SiX_3 π-bonding character progressively increases from X = H to F to Cl.[46b] This interpretation was confirmed by a vibrational analysis by Bürger[46d] of species of the $XMe_2Si-NH-SiMe_2X$ type, where it was found that the Si–N force constant (in mdyn/Å) progressively increases in the order X = Me (3.46), X = F (3.77), and X = Cl (3.86). On the other hand, substitution of the N–H hydrogen for methyl and trimethylsilyl groups leads to reduced Si–N force constants,[46d] due to the delocalization of the nitrogen lone pair in a third direction. With increasing trialkylsilyl substitution at nitrogen, for instance, the Si–N force constant (in

(41) (a) Natta, G.; Allegra, G.; Perego, G.; Zambelli, A. *J. Am. Chem. Soc.* **1961**, *83*, 5033. (b) Kushi, Y.; Fernando, Q. *J. Am. Chem. Soc.* **1970**, *92*, 91–96.
(42) (a) Davidson, N.; Brown, H. C. *J. Am. Chem. Soc.* **1942**, *64*, 316–324. (b) Ruff, J. K. *J. Am. Chem. Soc.* **1961**, *83*, 1798–1800. (c) Cucinella, S.; Salvatori, T.; Busetto, C.; Mazzei, A. *J. Organomet. Chem.* **1976**, *108*, 13–25. (d) See also: Wiberg, N.; Raschig, F.; Schmid, K. H. *J. Organomet. Chem.* **1967**, *10*, 29–40. (e) Sheldrick, G. M.; Sheldrick, W. S. *J. Chem. Soc. A* **1969**, 2279–2282.
(43) (a) Livingston, R. L.; Vaughan, G. *J. Am. Chem. Soc.* **1956**, *78*, 4866–4869. (b) Böhme, H.; Hilp, M. *Chem. Ber.* **1970**, *103*, 104–111. (c) Krabbenhoft, H. O.; Wiseman, J. R.; Quinn, C. B. *J. Am. Chem. Soc.* **1974**, *96*, 258–259 and references therein.
(44) Carlsen, N. R.; Radom, L.; Riggs, N. V.; Rodwell, W. R. *J. Am. Chem. Soc.* **1979**, *101*, 2233–2234.
(45) (a) Hencher, J. L.; Bauer, S. H. *J. Am. Chem. Soc.* **1967**, *89*, 5527–5529. (b) Glidewell, C.; Higgins, D.; Thomson, C. *J. Comput. Chem.* **1987**, *8*, 1170–1178.
(46) (a) Grosse-Ruyken, H.; Kleesaat, R. *Z. Anorg. Allg. Chem.* **1961**, *308*, 122–132. (b) Wannagat, U.; Behmel, K.; Bürger, H. *Chem. Ber.* **1964**, *97*, 2029–2036. (c) Mosconi, J. J.; MacDiarmid, A. G. *J. Chem. Soc., Chem. Commun.* **1965**, 307–308. (d) Bürger, H. *Monatsh. Chem.* **1966**, *97*, 869–878. (e) Wannagat, U.; Höfler, F.; Bürger, H. *Monatsh. Chem.* **1968**, *99*, 1186–1197. (f) Wannagat, U.; Bürger, H.; Höfler, F. *Monatsh. Chem.* **1968**, *99*, 1198–1204. (g) Airey, W.; Glidewell, C.; Robiette, A. G.; Sheldrick, G. M.; Freeman, J. M. *J. Mol. Struct.* **1971**, *8*, 423. (h) Klingebiel, U.; Meller, A. *Chem. Ber.* **1975**, *108*, 155–158.

mdyn/Å) decreases progressively from 4.0 in R_3SiNH_2 to 3.5 in $(R_3Si)_2NH$ to 3.2 in $(R_3Si)_3N$, compared to the normal Si–N single-bond value of 2.9.[46d]

Significant hyperconjugation at silicon of $n_N \rightarrow \sigma_{SiCl}^*$ type is seen in the experimentally determined gas-phase structure for (chlorosilyl)dimethylamine, $ClSiH_2N(CH_3)_2$:[47] The Si–Cl bond is parallel to the nitrogen lone pair, the geometry at N is very close to planar (in contrast to that for the silicon-unsubstituted species H_3SiNR_2, R = H, CH_3[35]), the Si–Cl bond is 0.02 Å longer than in H_3SiCl, and the Si–N bond length of 1.689 Å is 0.02–0.03 Å shorter than in other dimethyl(silyl)amines. Further experimental evidence for negative hyperconjugation at Si (and Ge, Sn) centers derives from studies of p-$((H_3C)_3A)_2C_6H_4$ compounds, where A = C, Si, Ge, Sn.[48] Even though Si, Ge, and Sn act as σ donors relative to C, they are found to act as π-acceptors in these para-disubstituted benzenes, lowering the symmetric π-orbital energies. Though it had been proposed that this effect could arise from back-donation from the ring π orbitals into d orbitals on Si, Ge, and Sn, it was shown by Giordon and Moore[48] to arise instead from hyperconjugation into σ^* orbitals at these atoms. Here, we have an example of $\pi_{CC} \rightarrow \sigma_{SiC}^*$ interaction. The importance of d orbitals at silicon has been questioned recently also by Rempfer et al.[49] Hyperconjugation into Si–H antibonds rather than bonding with Si 3d orbitals should be invoked as the origin of, for instance, the linearity of the SiNCS chain in H_3SiNCS.[50] We discuss other aspects of the generalized anomeric effect at silicon elsewhere.[2d]

D. N and O Centers. Experimentally observed conformations of R_2NNR_2 and ROOR species provide examples of the gauche effect.[1a,4] The tendency is for the lone pair orbitals (in the case of oxygen, the π-type lone pairs) of the central atoms to orient themselves at dihedral angles of roughly 60 or 90° to each other. Such gauche conformations are favorable for the most effective operation of negative hyperconjugation. Apparently, the only fluorine-substituted hydrazine that has been made is F_2NNF_2, and this species exists in gauche and anti conformers in roughly equal proportion.[51] This result is quite different from that of F_2NNH_2, where our calculations find that gauche is strongly favored, and it could be that the N–F dipoles play an important role in stabilizing the anti conformer of F_2NNF_2. Interestingly, Shvo[51] points out that the application of the "gauche rule"[4] to the case of $FNHNH_2$ wrongly predicts that the favored conformation should have the lone pair of NH_2 gauche to both the lone pair of FNH and to the N–F bond (in our notation, S-st instead of A-st), as this leads to the maximum number of gauche lone pair–lone pair and lone pair–polar bond configurations. Another relevant example is $(F_3C)_2NN(CF_3)_2$, which is found experimentally to have very nearly planar nitrogen atoms and a dihedral CNNC angle close to 90°.[52] Here, $n_N \rightarrow \sigma_{CF}^*$ interaction into the CF_3 groups (as in F_3CNH_2) apparently effects a planarization of the two nitrogen centers. This planarization also favors stronger $n_N \rightarrow \sigma_{NC}^*$ interaction across the N–N bond, as reflected in the experimentally observed reduction of the N–N distance by 0.05 Å with respect to that in H_2NNH_2. An anomeric effect at N has been observed in the studies of Nelsen[53] on cyclic tetraalkylhydrazines, where a $-N(CH_3)-N(CH_3)-$ unit is imbedded in a six-membered ring and $n_N \rightarrow \sigma_{NC}^*$ interaction occurs. With regard to oxygen centers, a relevant example is FOOF,[54] which is found experimentally to have a dihedral angle of 88.5° and unusually short O–O (1.22 Å) and long O–F (1.58 Å) bond lengths.[54a] Though electron correlation effects due to the large number of lone pairs in this species are quite strong,[54b,c] hyperconjugation from the oxygen p-type lone pairs into the O–F antibonds certainly plays a partial role in the unusual bond lengths; Ahlrichs and Taylor[54c] presented a contour diagram of the localized molecular orbital for the oxygen lone pair in FOOF that showed this hyperconjugation. NBO analysis of this molecule at the HF/6-31G* level confirms that significant $\pi_O \rightarrow \sigma_{OF}^*$ interaction occurs in this species, the amount of donation into each σ_{OF}^* orbital being 0.05e.

E. P Centers. In addition to the structure of F_2PNH_2 (section III-E), a microwave structure has been also determined for the substituted species $F_2PN(CH_3)_2$,[55] which was found to exist in the same conformation, with a nearly planar nitrogen atom. The P–N distance was found to be 0.01 Å longer, at 1.66 Å. No rotation barrier for $F_2PN(CH_3)_2$ could be determined by NMR[56] (just as in the case of F_2PNH_2[21]); upper limits for this barrier of 8[56a] and 7 kcal/mol[56b] were set (consistent with our calculated barrier of 6 kcal/mol for F_2PNH_2 from Table IV). Another interesting case involves the anticancer drug cyclophosphamide, or Endoxan[57] (in which the exo-anomeric effect operates[1a]):

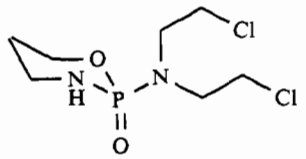

The crystal structure of this drug is analogous to that of the F_2PNR_2 compounds mentioned above: the geometry at the exocyclic nitrogen is essentially planar ($\Delta\theta(N) = 0.1°$), the P–N distance is 1.63 Å, and the PNR_2 plane bisects the plane involving the ring atoms O–P–N. The system is thus set up for strong $n_N \rightarrow \sigma_{PO}^*$ and $n_N \rightarrow \sigma_{PN}^*$ interactions. Finally, it is to be mentioned that extensive evidence for anomeric effects at phosphorus centers exists (involving $n_N \rightarrow \sigma_{PX}^*$ or $n_O \rightarrow \sigma_{PX}^*$ hyperconjugation); the extent of this evidence is larger than that for any other noncarbon center.[1a,c,58]

F. S Centers. To our knowledge, no fluorosulfenamides $FSNR_2$ have ever been prepared. Nevertheless, large torsional barriers have been found in many other sulfenamides, as has been reviewed by Raban and Kost.[28b] Rotational barriers in *N,N*-dialkyl-substituted $ClSNR_2$ compounds range from 14.5 to 15.5 kcal/mol.[28b] The species $ClSNCH_3CH_2Ph$

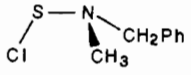

for instance, is estimated by NMR to have a rotation barrier (ΔG^*) of 15.5 kcal/mol, which compares favorably with the theoretical rotation barrier of 15.9 kcal/mol obtained for $ClSNH_2$ in this work. A nearly planar geometry at N is observed in *N*(1-(1-naphthyl)-1-ethyl)-*N*-(phenylsulfonyl)trichloromethanesulfenamide:[59]

(47) Anderson, D. G.; Blake, A. J.; Cradock, S.; Ebsworth, E. A. V.; Rankin, D. W. H.; Welch, A. J. *Angew. Chem.* **1986**, *98*, 97–99.
(48) Giordon, J. C.; Moore, J. H. *J. Am. Chem. Soc.* **1983**, *105*, 6541–6544.
(49) Rempfer, B.; Oberhammer, H.; Auner, N. *J. Am. Chem. Soc.* **1986**, *108*, 3893–3897.
(50) Jenkins, D. R.; Kewley, R.; Sugden, T. M. *Trans. Faraday Soc.* **1962**, *58*, 1284–1290.
(51) Shvo, Y. In *The Chemistry of the Hydrazo, Azo and Azoxy Groups*; Patai, S., Ed.; Wiley: New York, 1975; pp 1017–1095.
(52) Bartell, L. S.; Higginbotham, H. K. *Inorg. Chem.* **1967**, *4*, 1346–1350.
(53) Nelsen, S. F. *Acc. Chem. Res.* **1978**, *11*, 14–20. See also ref 1a.
(54) (a) Jackson, R. H. *J. Chem. Soc.* **1962**, 4585–4592. (b) Rohlfing, C. M.; Hay, P. J. *J. Chem. Phys.* **1987**, *86*, 4518–4522 and references therein. (c) Ahlrichs, R.; Taylor, P. R. *Chem. Phys.* **1982**, *72*, 287–292. (d) Theoretical models of FOOF have been discussed by: Burdett, J. K.; Lawrence, N. J.; Turner, J. J. *Inorg. Chem.* **1984**, *23*, 2419–2428.
(55) Forti, P.; Damiani, D.; Favero, P. G. *J. Am. Chem. Soc.* **1973**, *95*, 756–759.
(56) (a) Cowley, A. H.; Dewar, M. J. S.; Jackson, W. R.; Jennings, W. B. *J. Am. Chem. Soc.* **1970**, *92*, 5206–5213. (b) Gouesnard, J. P.; Dorie, J.; Martin, G. J. *Can. J. Chem.* **1980**, *58*, 1295–1304.
(57) Clardy, J. C.; Mosbo, J. A.; Verkade, J. G. *J. Chem. Soc., Chem. Commun.* **1972**, 1163. Garcia-Blanco, S.; Perales, A. *Acta Crystallogr., Sect. B: Struct. Crystallogr. Cryst. Chem.* **1972**, *B28*, 2647–2652.
(58) Fanni, T.; Taira, K.; Gorenstein, D. G.; Vaidyanathaswamy, R.; Verkade, J. G. *J. Am. Chem. Soc.* **1986**, *108*, 6311–6314 and references therein.
(59) (a) Kay, J.; Glick, M. D.; Raban, M. *J. Am. Chem. Soc.* **1971**, *93*, 5224–5229. (b) Clearly, hyperconjugation from n_N to both sulfur atoms occurs, $n_N \rightarrow \sigma^*(S–C)$ and $n_N \rightarrow 2\sigma^*(S–O)$. This induces near planarity at N. The $N–SO_2$ bond is lengthened by strong $2\pi(O) \rightarrow \sigma^*(S–N)$ interaction, and this plays a role in the discrepancy between the two S–N bond lengths.

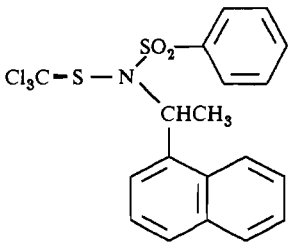

The S–N bond of the $NSCCl_3$ unit is significantly shorter than the S–N bond of the NSO_2Ph unit (1.643 vs 1.713 Å),[59b] and $\Delta\theta(N)$, the amount of pyramidalization at N, is 3.5°. This compound is significantly closer to planarity at N than $FSNH_2$ and $ClSNH_2$, which in our calculations have $\Delta\theta(N)$ values of 12–13°. Raban and Kost have rationalized the large rotation barriers of sulfenamides on the basis of negative hyperconjugation,[28b] supporting their conclusion by ab initio calculations on model species of RCH_2NH_2 type (R = H, F, NH_3^+).[28a] Our results are consistent with their work. It is therefore unnecessary and misleading to invoke π-bonding with d orbitals on sulfur in explanations of rotation barriers or features of NMR spectra of selfenamides, as has been done recently.[28c]

Another case of strong $n_N \rightarrow \sigma_{SCl}^*$ interaction is the $ClSNSCl^+$ cation,[60] which has a cis geometry with very large SNS and NSCl angles of 151 and 110.6°, respectively. This assertion is confirmed by our NBO analysis of this cation at the 3-21G(*) level at the experimental geometry, which shows that the nitrogen in-plane lone pair has 87% p character and donates 0.15e to the σ_{SCl}^* orbitals. Of the donated 0.15e, only 0.018e goes into sulfur d orbitals. The S–N distance in $ClSNSCl^+$ is much shorter than would be expected on the basis of the SNS angle, which led Banister and Durrant[61] to question the validity of the experimental structure. (The X-ray structure of the cation has been reconfirmed.[60]) The strong $n_N \rightarrow \sigma_{SCl}^*$ interaction would certainly play a role in the unusually short S–N bond length (1.528 Å), and interaction of n_N with the sulfur d orbitals is only of minor importance, in contrast to what was assumed by Banister and Durrant.[61]

G. Extension to Hypervalent Molecules. In addition to F_3C-NH_2, Klöter and Seppelt[23b] have synthesized the related alcohol F_3COH, which similarly is unstable with respect to loss of HF. This perfluorinated alcohol is rather acidic, and its corresponding base F_3CO^- can form stable salts with bulky counterions. The O^- substituent, having two π-type lone pairs and a charge of −1, is a significantly more powerful electron donor than NH_2, and the $\pi_O \rightarrow \sigma_{CF}^*$ interaction in F_3CO^- is so strong that the C–O bond length is only 1.23 Å,[7b] a value typical for a C=O double bond. This anion is thus *geometrically* hypervalent, since, by geometric criterion, it has a structure of form $[F_3C{=}O]^-$ where carbon is "pentavalent". A similar situation occurs in F_3NO,[7a] which *geometrically* is not to be represented as a semipolar amine oxide but as $F_3N{=}O$. The strength of hyperconjugation interactions is certainly not weaker at second-row centers such as P and S, in species such as F_3PO, PO_4^{3-}, F_3SN, SO_4^{2-}, and $(H_3C)_2SO_2$, which are valence isoelectronic with F_3CO^-. Here, donations into central atom d orbitals become more important than in F_3CO^-, F_3NO, or any of the nonhypervalent species treated in this work. Nevertheless, NPA and NBO analysis of such systems shows that negative hyperconjugation is still several times stronger than delocalization into central-atom d orbitals.[62]

V. Conclusions

This work demonstrates how fluorine substitution influences conformational preferences, A–N bond lengths, and barriers to internal rotation and inversion of amines through $n_N \rightarrow \sigma_{AF}^*$ hyperconjugation. All of these changes are consistent with the generalized anomeric effect. Variations in A–N "single" bond lengths of up to 0.15 Å have been found, in comparisons of various conformers of nonfluorinated and fluorinated amines. Parts of these variations are independent of conformation and are due to electrostatic effects.[2c] As in our study of the polyfluorinated hydrides,[2c] the generalized anomeric effect at B and Al centers is weak (but noticeable), stronger at Si centers, and strongest at C, N, P, and S. In this study, a strong anomeric effect at O is also found, in spite of the high electronegativity of O. This is partly due to the weakness of O–F bonds and hence low energy of the σ_{OF}^* orbital. Examples of alterations in the energy ordering of conformers are the following:[63] Fluorine substitution of $HONH_2$ (to give $FONH_2$) reverses the syn–anti preference, and fluorine substitution of $HSNH_2$ (to give $FSNH_2$) results in the disappearance of a minimum for the anti conformer; just as for $FSNH_2$, and in contrast to the case for $FNHNH_2$, $FPHNH_2$ has only a single minimum conformation. In contrast to the case for ethane, a minimum (though shallow) exists for the *eclipsed* C_s conformer of FCH_2NH_2. In F_2CHNH_2, the eclipsed C_s form is lower in energy than the staggered C_s form (these are both transition structures with respect to internal rotation of the C_1 minimum structure). In F_2PNH_2, the syn–anti preference is the reverse of that in H_2NNH_2 and in H_2PNH_2 (both syn and anti are transition structures for internal rotation). Significant $n_N \rightarrow \sigma_{AH}^*$ hyperconjugation also occurs in many of these species, partially masking the effects of $n_N \rightarrow \sigma_{AF}^*$ interactions. In $FONH_2$ and $FSNH_2$, however, no A–H bonds are present and the unmasked $n_N \rightarrow \sigma_{AF}^*$ interaction manifests itself in very large rotation barriers of 12 and 18 kcal/mol, respectively.

Due to its particularly large rotation barrier, $FSNH_2$ was singled out for detailed analysis using the natural bond orbital (NBO)[13] method. The NBO analysis showed that the generalized anomeric effect in $FSNH_2$ (both energetic and geometric aspects) can be interpreted rather quantitatively in terms of negative hyperconjugation, primarily of $n_N \rightarrow \sigma_{SF}^*$ type and secondarily of $\pi_S \rightarrow \sigma_{NH}^*$ type. Workers who promote other models for the origin of the anomeric effect are encouraged to test these out quantitatively on $FSNH_2$. We are confident, however, that negative hyperconjugation will stand as the best and simplest explanation of the anomeric effect. Chemical bonding has its origin in interatomic *orbital* interactions, and the bond length and angle changes associated with the anomeric effect are most naturally discussed in terms of changes in the form and occupancy of localized bonding, lone pair, and antibonding orbitals, as in the negative hyperconjugation model.

An additional important result from our work is that negative hyperconjugation in the nonhypervalent species studied here is on the order of 5–10 times more important than p–d bonding with d orbitals of second-row atoms. The role of d orbitals in such nonhypervalent systems should no longer be emphasized as it has been up to now;[64] negative hyperconjugation at Si, P, and S (and Cl) centers provides ample opportunity for these atoms to participate in π-type bonding interactions beyond those allowed by strict application of the octet rule. Since negative hyperconjugation plays such an important role in the amine species discussed in this work, it is also misleading to discuss their geometries purely in terms of nonbonded (repulsive) contact distances, as had been done by Glidewell,[65] although such considerations obviously are of importance.

For F_2BNH_2 and F_2PNH_2, the fluorinated amines studied in this work whose structures have been experimentally determined, good agreement is obtained between theory and experiment. The

(60) Glemser, O.; Mews, R. *Angew. Chem.* **1980**, *92*, 904–921.
(61) Banister, A. J.; Durrant, J. A. *J. Chem. Res., Miniprint* **1978**, 1912.
(62) Reed, A. E.; Schleyer, P. v. R., manuscript in preparation.
(63) The general topic of the influence of chemical substitution on the number and types of stationary points of molecules has been discussed recently by: Ángyán, J. G.; Daudel, R.; Kucsman, Á.; Csizmadia, I. G. *Chem. Phys. Lett.* **1987**, *136*, 1–12.
(64) See, e.g., ref 21, 28c, 41a,b, 46d, 47, 50, 56b, and 61. Often, any significant deviation of bond lengths from those predicted by the Schomaker–Stevenson relation[37] has been taken as "evidence" for the participation of d orbitals. An extensive bibliography of works raising the question of d-orbital involvement in the chemistry of nonhypervalent (and hypervalent) species is given by: Kwart, H.; King, K. G. *d-orbitals in the Chemistry of Silicon, Phosphorous and Sulfur*; Springer: Berlin, 1977.
(65) Glidewell, C. *Inorg. Chim. Acta* **1975**, *12*, 219–227.

results of this study have relevance far beyond the specific class of fluorinated amines treated here theoretically, however, and the conceptual connections of this work with a broad range of main-group chemical species in which negative hyperconjugation can play an important role in stabilizing ground or transition structures was hinted at in our discussion in section IV. Furthermore, our earlier conclusions[2a,66] concerning the general phenomenon of negative hyperconjugation have been reconfirmed and extended.

Acknowledgment. This work was supported by the Deutsche Forschungsgemeinschaft, Fonds der Chemischen Industrie, the Bundesministerium für Forschung und Technik, and Convex Computer Corp. A study of $FSiH_2NH_2$ was suggested by Prof. Epiotis, whom we thank for his stimulation.

Registry No. $HBeNH_2$, 50688-89-6; $FBeNH_2$, 116377-34-5; H_2BNH_2, 14720-35-5; $FBHNH_2$, 116377-35-6; F_2BNH_2, 50673-31-9; H_3CNH_2, 74-89-5; FCH_2NH_2, 36336-09-1; F_2CHNH_2, 47950-15-2; F_3CNH_2, 61165-75-1; H_2NNH_2, 302-01-2; $FNHNH_2$, 36336-10-4; F_2NNH_2, 115967-51-6; $HONH_2$, 7803-49-8; $FONH_2$, 36405-65-9; $HMgNH_2$, 116377-36-7; $FMgNH_2$, 116377-37-8; H_2AlNH_2, 53138-60-6; $FAlHNH_2$, 116377-38-9; F_2AlNH_2, 116377-39-0; H_3SiNH_2, 13598-78-2; $FSiH_2NH_2$, 116377-40-3; F_2SiHNH_2, 116377-41-4; F_3SiNH_2, 116377-42-5; H_2PNH_2, 13598-67-9; $FPHNH_2$, 14616-21-8; F_2PNH_2, 25757-74-8; $HSNH_2$, 14097-00-8; $FSNH_2$, 36579-30-3; $ClSNH_2$, 13812-03-8.

Supplementary Material Available: GAUSSIAN 82 archive entries (same format as in ref 32a) of the HF/6-31G* and MP2FU/6-31G* geometry optimizations, HF/6-31G* frequency, and MP2FC/6-31G* and MP4SDTQ/6-31+G* energy calculations performed in this work, the complete geometries being specified (22 pages). Ordering information is given on any current masthead page.

(66) Reed, A. E. Ph.D. Thesis, University of Wisconsin, Madison, WI, 1985.

Contribution from the Institut für Organische Chemie der Friedrich-Alexander-Universität Erlangen-Nürnberg, Henkestrasse 42, D-8520 Erlangen, Federal Republic of Germany

Dilithiodiborane(6) ($Li_2B_2H_4$): An Experimentally Viable Species with a B=B Double Bond. Planar No-Bond–Double-Bond Isomers with Pentacoordinate Boron?†

Elmar Kaufmann* and Paul von Ragué Schleyer

Received March 14, 1988

The title compound **6a**, the all-planar dilithium derivative of the tetrahydrodiborate(2–) dianion, $B_2H_4^{2-}$, is calculated to be a highly stable species thermodynamically with a B=B double bond of length 1.613 Å (6-31G* data). All possible decomposition reactions are endothermic, and the dissociation energy ($Li_2B_2H_4 \rightarrow 2LiBH_2$) is 117.9 kcal/mol (MP2/6-31G*//6-31G* + ZPE). Other isomers of dilithiodiborane(6), $Li_2B_2H_4$, which correspond to minima, are derivatives of diborane(6), B_2H_6, with both lithiums in terminal (**5**) or in bridging (**4a**) positions. Their relative energies are 77.9 and 82.9 kcal/mol, respectively (MP2/6-31G*//6-31G* + ZPE). Attractive ("agostic") Li–H interactions are responsible for the planar conformations of **6a** and **4a**. The barrier for converting **4a** into **6a** ("no-bond–double-bond isomerism", a form of bond-stretch isomerism) is too small (only 4.9 kcal/mol at MP2/6-31G*//6-31G* + ZPE) to be able to predict the existence of **4a**.

Introduction

Since the basic work of Stock[1] the number of known boron hydrides and hydroborate anions has been growing extensively, including compounds containing up to 30 boron atoms.[2] Most of them are characterized by delocalized multicenter bonds because of their electron-deficient nature. However, despite the variety of their structures, none of them have been found to exhibit a boron–boron double bond.

The simplest molecule expected to have such a boron–boron π-bond is diborane(2), B_2H_2. Theoretical studies[3-5] indicate its ground state to be a triplet[5] with the two degenerate π orbitals singly occupied. Experimentally, only nonstoichiometric polymeric $(BH_x)_n$ compounds are known with x close to 1.[6] The polymerization energy of B_2H_2 has been calculated to be about 260 kcal/mol.[4] Formal halogen derivatives of B_2H_2 are "oligomeric" and have cluster structures, e.g., B_nCl_n (n = 4, 8, 9).[7] However, the ion $B_2Cl_2^+$ has been observed in the mass spectral fragmentation of B_2Cl_4,[8a] and the doubly charged ion B_2^{2+} has been produced in a metastable state in a tandem accelerator.[9] Koch et al.[10] examined the helium-substituted derivative B_2He_2 calculationally but did not find it to be a minimum. A less "exotic" approach to a B=B π-bond was suggested quite recently theoretically by Jouany, Barthelat, and Daudey:[5] Substitution of H in B_2H_2 by amino groups should lead to the singlet-ground-state molecule $H_2NB{=}BNH_2$, isoelectronic with butatriene, $H_2C{=}C{=}C{=}CH_2$. However, no boron–boron double bond with dicoordinated boron has been characterized experimentally. The reason seems to be the extreme electrophilic nature of structures of type **1** (which also may be represented as having two partial π-bonds).

—B=B— or —B⋯B—

1

Compounds involving boron and exhibiting double-bond character are known with, e.g., nitrogen and phosphorus.[11] There

† Dedicated to Prof. H. Nöth on the occasion of his 60th birthday.

(1) Stock, A. *Hydrides of Boron and Silicon*; Cornell University Press: Ithaca, NY, 1933 (reissued 1957).
(2) (a) *Gmelin Handbook of Inorganic Chemistry*; Springer-Verlag: New York, 1987; Boron Compounds 1, 3rd suppl. (b) We follow the nomenclature of boron compounds approved by the Council of the American Chemical Society: *Inorg. Chem.* **1968**, *7*, 1945. E.g., B_2H_4 will be diborane(4), B_2H_6 diborane(6), $B_2H_3^-$ trihydrodiborate(1–), etc.
(3) Dill, J. D.; Schleyer, P. v. R.; Pople, J. A. *J. Am. Chem. Soc.* **1975**, *97*, 3402. Also see: Bigot, B.; Lequan, R. M.; Devaquet, A. *Nouv. J. Chim.* **1978**, *2*, 449.
(4) Armstrong, D. R. *Theor. Chim. Acta* **1981** *60*, 159.
(5) Jouany, C.; Barthelat, J. C.; Daudey, J. P. *Chem. Phys. Lett.* **1987**, *136*, 52.
(6) Köster, R. *Angew. Chem.* **1958**, *70*, 743.
(7) (a) Atoji, M.; Lipscomb, W. N. *Acta Crystallogr.* **1953**, *6*, 547. (b) Jacobson, R. A.; Lipscomb, W. N. *J. Chem. Phys.* **1959**, *31*, 605. (c) Kane, J.; Massey, A. G. *J. Inorg. Nucl. Chem.* **1971**, *33*, 1195. Lanthier, G. F.; Kane, J.; Massey, A. G. *J. Inorg. Nucl. Chem.* **1971**, *33*, 1569.
(8) (a) Dibeler, V. H.; Walker, J. A. *Inorg. Chem.* **1969**, *8*, 50. (b) Dibeler, V. H.; Liston, S. K. *Inorg. Chem.* **1968**, *7*, 1742. Also see: Bews, J. R.; Glidewell, C. *THEOCHEM* **1982**, *6*, 333.
(9) Galindo-Uribarri, A.; Lee, H. W.; Chang, K. H. *J. Chem. Phys.* **1985**, *83*, 3685.
(10) Koch, W.; Frenking, G.; Gauss, J.; Cremer, D.; Collins, J. R. *J. Am. Chem. Soc.* **1987**, *109*, 5917.
(11) (a) For recent examples see: (a) Bartlett, R. A.; Feng, X.; Olmstead, M. M.; Power, P. P.; Weese, K. J. *J. Am. Chem. Soc.* **1987**, *109*, 4851. Paetzold, P.; von Plotho, C.; Schmid, G.; Boese, R. *Z. Naturforsch., B: Anorg. Chem., Org. Chem.* **1984**, *39B*, 1069. Paetzold, P.; von Plotho, C.; Schmid, G.; Boese, R.; Schrader, B.; Bougeard, D.; Pfeiffer, U.; Gleiter, R.; Schäfer, W. *Chem. Ber.* **1984**, *117*, 1089. (b) Bartlett, R. A.; Feng, X.; Power, P. P. *J. Am. Chem. Soc.* **1986**, *108*, 6817.

0020-1669/88/1327-3987$01.50/0